Impulse response analysis of neuromodulation for the treatment of motor symptoms in Parkinson's disease

Staffan Hedström

LUND UNIVERSITY

Department of Automatic Control

MSc Thesis
ISRN LUTFD2/TFRT--5993--SE
ISSN 0280-5316

Department of Automatic Control
Lund University
Box 118
SE-221 00 LUND
Sweden

Printed in Sweden by Tryckeriet i E-huset
Lund 2016

Abstract

In adaptive deep brain stimulation, a treatment for motor symptoms in Parkinson's disease, the target of the stimulus is usually in the sub-thalamic nucleus or the globus pallidus. In this thesis, a new stimulus target called reticular thalamus is investigated in a rat model of Parkinson's disease. The responses to the stimulus were recorded from both local field potentials and action potentials from neurons in a live animal implanted with an electrode array and stimulus electrode. The local field potentials were used to investigate the state of a rat, to categorise healthy, parkinsonian and dyskinetic states, to create a response to the stimulus used for investigating the effects of the new stimulus target and to try find the transfer function (turns input into output) to the brain of a rat model of Parkinson's disease with the Markov parameter realisation algorithm. The new stimulus target showed interesting and clear visual responses from the rat and set the structures in the basal ganglia in a 5-10 Hz ringing for half a second as revealed by a peristimulus time histogram. A power spectral density diagram revealed characteristics previously shown to be correlated with Parkinson's disease. The transfer function created from the responses was not able to predict the responses to other stimulation protocols other than the one used to build the transfer function, possibly due to the fact that the stimulus target was more effectively inhibited by the higher frequency stimulus protocols, so that the biological properties changed the system.

Acknowledgements

Here I'd like to thank the many people I've had around me during the time I worked on this project.

Big thanks and warm hugs to my eternal friend who have help motivate me, brainstorm and help getting me out of bed those mornings when it's just to hard get out of it. The bed was calling to me but so were you ;). So thank you Joel Sjöbom for helping me through this and all the lovely time we spend on discussing all the tiny math and programming problems we both encountered!

I would also like to say my warmest of thanks Inga Rún Helgadóttir, my love and life companion. You have helped me much the way Joel have with motivation, inspiration, pushing me forward and pulling me back up after falling.

Next up is my supervisors. Thank you Per Petersson and Rolf Johansson for your patience with me and allowing me to take the time that was needed. Thank you Per for you everlasting positive outlook and fast responses in the middle of the night. And thanks to you Rolf for your honesty and straightforwardness.

Thanks to PhD student Nela Ivica and master student Rikard Nilsson for being great in assisting with stuff around the lab. Nela Ivica for providing instructions about everything in the lab and its equipment, Rikard for being a good lab partner freely giving all the biological expertise I as an engineering student lacked such as surgery and animal care. Thanks to both for being so friendly and being part of the the building blocks of the good atmosphere at NRC.

Thanks to the post docs Pär Halje and Ulrike Richter. Pär and Ulrike have written or helped develop a lot of the help scripts I've been using and giving good instructions on how to use them. They have also both been part of brainstorming and discussions of my work and results. Extra thanks to Pär for also taking some extra time with assisting with the production of the thesis, criticising and looking through the results.

Contents

1. Introduction **1**
1.1 Ethics 2

2. Background **3**
2.1 Parkinson's disease 3
2.2 DBS and aDBS 6
2.3 Objectives 8
2.4 Limitations 9

3. Equipment and Experiments **10**
3.1 Electrode and DBS placement 10
3.2 Data acquisition and stimulus generator 11
3.3 Stimulation protocol 12
3.4 Threshold testing 13
3.5 Recording data procedure 13

4. Methods **14**
4.1 Signal approximation assumptions 14
4.2 Yield of channels and normalisation 14
4.3 Finding time stamps 17
4.4 Evoked potentials 20
4.5 Peristimulus time histogram 21
4.6 Spectral Analysis 23
4.7 System Identification 25
4.8 Validation of model 29

5. Results **30**
5.1 Threshold testing and observations of visual behaviour 30
5.2 Power density spectra of LFPs 30
5.3 Evoked potentials 32
5.4 PSTH of evoked action potentials 36
5.5 Markov realisation model responses 37

6. Discussion **45**
6.1 Categorising data and power spectral densities 45
6.2 Evoked potentials 45
6.3 Peristimulus time histograms 45
6.4 Markov model responses, order and Bode diagrams 46
6.5 Improving results 47
6.6 Alternative methods 48
6.7 Objectives and comments 48
6.8 Conclusion 49
Appendix **50**
Bibliography **53**

1

Introduction

One treatment for the motor symptoms of Parkinson's disease (PD) is deep brain stimulation (DBS) in which an electrode is implanted into the patient's brain. The process of finding the right stimulus parameters can be quite long and arduous. The optimal parameters for the treatment are often individual to each patient and may also change with time. Therefore, researchers are now experimenting with adaptive deep brain stimulation in which a feedback loop is used to change parameters and adapt to the patient's individual state. One challenge with this approach is finding a suitable control variable. Previous studies have used power spectral density peak thresholds [Little et al., 2013] while another investigated spikes in the globus pallidus or primary cortex [Rosin et al., 2011].

The basal ganglia are a collection of brain structures (see figures 2.1 and 2.2(b)) of the brain important for initiating and stopping movement and plays a significant role in the motor symptoms of PD [Kringelbach et al., 2010]. There is still much unknown regarding the function of DBS in treating PD. The usual targets for DBS are the sub-thalamic nucleus or the globus pallidus [Kringelbach et al., 2010], which are both part of the basal ganglia. The main objective in this master's thesis was to investigate how the basal ganglia react to stimuli in the reticular thalamus and how to identify a model for closed-loop DBS. It was hypothesised by the author of this master's thesis that the model would be able to predict how the local field potentials (LFPs) of structures in the basal ganglia react to different kinds of stimuli making healthy LFP signals the ideal control variable. To reach this goal 6-OHDA lesioning, a rat model of PD, was used which leaves one hemisphere of the brain intact and the other hemisphere is lesioned (damaged) in a way that makes it display parkinsonian motor symptoms.

To verify that the rat was parkinsonian the LFPs of three different states were recorded: healthy (intact hemisphere), parkinsonian and L-dopa induced dyskinetic. To determine how the basal ganglia reacted to stimulation, peristimulus time histograms and evoked potentials (reactions in LFPs from a stimulus pulse) were created and inspected. The evoked potentials were interpreted as the system

impulse response and, thus, they were used in the Markov parameter realisation algorithm to create a discrete-time transfer function. Responses to two stimulation frequencies were simulated and recorded and were compared to see how well the model performed. Also the bode diagrams (frequency responses, describing gain and phase shift) were compared to the power spectral density plot to look for similarities.

1.1 Ethics

All tests were performed on Sprague Dawley rats at Biomedical Centre in Lund by PhD students and the author with the supervision of a mentor. The rats were kept in a 12 hour day, 12 hour night cycle and had free continuous access to food and water. All experiments were conducted with the approval of the Malmö/Lund Ethical Committee on Animal Research.

2

Background

2.1 Parkinson's disease

Parkinson's disease (PD) is a chronic progressive movement disorder. The Parkinson's Disease Foundation (PDF) states that the underlying cause of this neurodegenerative disease is the death and or malfunction of neurons (nerve cells in the brain). Primarily neurons in the midbrain that are responsible for the production of dopamine are affected. Dopamine is a neurotransmitter that modulates neuronal activity that controls movement [PDF, 2015b]. As a result of neuronal death, some movement controlling structures will have a lack of dopamine and be unable to function properly. This leads to the development of parkinsonian motor symptoms. Examples include:

- **tremors:** of the hands, arms, legs, jaw and face
- **bradykinesia:** slowness of movement
- **rigidity:** stiffness of the limbs and trunk
- **postural instability:** leads to impaired balance and coordination [PDF, 2015b].

Approximately 1% of the population over the age of 65 years is afflicted by this disease. Although symptoms can be effectively treated for the first few years, side-effects from the medication and incomplete therapeutic effect lead to the gradual worsening of symptoms.

Basal Ganglia Circuit

The reduced amounts of dopamine production in the midbrain strongly affect the basal ganglia circuit. In the early stage of the disease, the neurons mostly die in a substructure of substantia nigra called substantia nigra pars compact (SNc) which supplies the basal ganglia with dopamine [Kim et al., 2003]. The basal ganglia are important in motor control and it's anatomical location can be seen in Figure

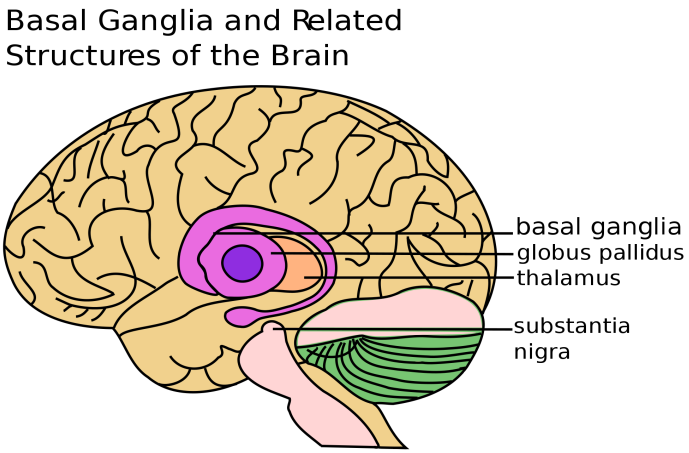

Figure 2.1 Illustrative figure on the basal ganglia's anatomical placement in the human brain. Here, some of the brain structures are shown that are included in the basal ganglia circuit, like the globus pallidus, thalamus and the substantia nigra. Figure credit to [Leevanjackson, 2009].

2.1. The basal ganglia are also involved in other non-motor functions, however, the focus for this thesis is the motor symptoms associated with PD. During movements and in anticipation of movements, the neurons in the basal ganglia are involved and are required for the normal course of voluntary movements [Purves, 2004]. When the SNc is damaged and dopamine production is reduced, the normal course of movements is hindered. The resulting abnormal circuit functions affect all structures in the basal ganglia as well as the cortex and thalamus, making motor control less effective. In practice, this means that patients with PD have problems sending commands that initiate and terminate a movement, making it difficult to switch smoothly between motor states [Purves, 2004]. The initial conceptual model of the basal ganglia can be seen in Figure 2.2 (a). Here, the basal ganglia communicate through the thalamus with the motor cortex which sends signals to the spinal cord. In this model, it was hypothesised that the flow of dopamine from the SNc only affected two types of dopamine receptors in the striatum, one which inhibits the indirect pathway and the other which sends excitatory signals to the direct pathway, both ultimately leading to less motor activation. However, recent studies have shown that the model is more complex and the input/output is hard to predict [Redgrave et al., 2010]. Figure 2.2 (b) shows a significantly more complex network connectivity where also the reticular thalamus is introduced into the circuitry.

The neurons and structures in the basal ganglia also communicate with a

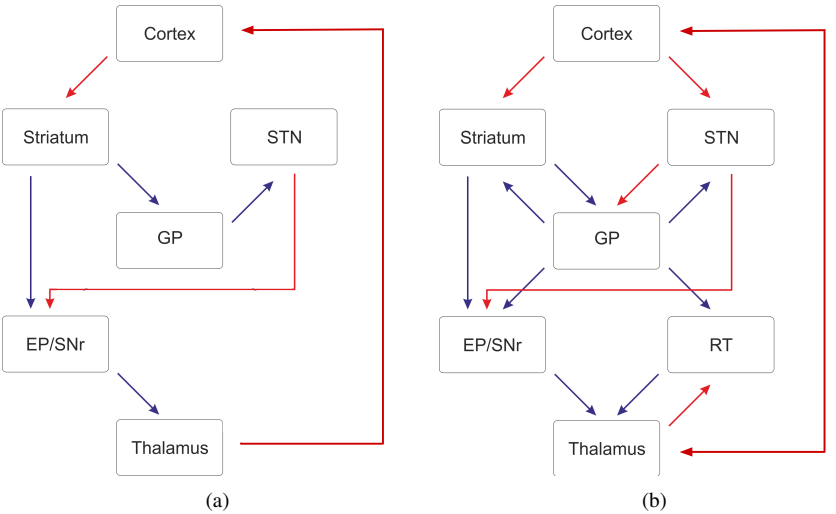

Figure 2.2 (a) The initial model of basal ganglia. The input can be seen as the signals from the cortex and the output from the basal ganglia can be seen as the input to the thalamus. Red: inhibitory signals (glutamate). Blue: excitatory signals (GABA). In this model the input is the signal from the cortex to the striatum and the output is the inhibitory signal from the thalamus to the cortex. The focus in this model lies in the relationship between the direct pathway (striatum $\rightarrow$ SNr $\rightarrow$ thalamus) and the indirect pathway (striatum $\rightarrow$ GP $\rightarrow$ STN $\rightarrow$ SNr $\rightarrow$ thalamus). (b) The more complex version of basal ganglia revealed in recent studies instead of just the striatum having dopamine receptors, all structures have it, making the system harder to predict and no longer follow the simple path of a direct and indirect pathway. Also here the reticular thalamus (RT) have been added. Abbreviations: EP, entopenduncular; GP, globus pallidus; RT, reticular thalamus; SNr, substantia nigra pars reticulata; STN, subthalamic nucleus. This figure is a modified version of [Redgrave et al., 2010].

complex call and response of activity in other areas of the brain, including the thalamus and cortex [Kringelbach et al., 2010]. These oscillations of activity are quite precise and need to be in synchronisation for our motor control to function quickly and fluidly [Kringelbach et al., 2010]. When neurons die, some structures in the basal ganglia weaken and may not be able to keep up their part of the oscillatory activity [Kringelbach et al., 2010]. Interesting frequencies can be found in the oscillation between the basal ganglia and cortex. Some of these oscillations have been categorised according to the part of movement control they are involved in as shown in Table 2.1. [Kringelbach et al., 2010]. In patients with PD, an increase in the antikinetic oscillation (11-30 Hz) and partial or complete suppression of prokinetic oscillations (60-80 Hz) have been observed [Kringelbach et al., 2010]. It is also worth mentioning, that with an increase in muscle activity, say from lying

Tremor related	3-11 Hz	(theta band)
antikinetic	11-30 Hz	(beta band)
prokinetic	60-80 Hz	(gamma band)

Table 2.1 Neuron oscillation frequencies and their relation to motor control.

still to running, there is naturally an increase in the activity of the neurons in the basal ganglia. This can lead to a broad banded increase of the oscillations of the basal ganglia.

Levodopa

The cause of the parkinsonian motor symptoms is largely due to the lack of dopamine. The treatment of PD is however not simply to give a patient dopamine because of the blood-brain barrier (BBB). The BBB is a diffusion barrier that selectively excludes most blood-borne substances from entering the brain [Ballabh et al., 2004], the BBB allows the brain to protect itself from blood-borne neurotoxins and simultaneously allows the passage of nutrients. Most of the neurotransmitters, including dopamine, are part of the excluded substances [Dash, 1997]. Levodopa (L-dopa) is a precursor to dopamine and can cross through the BBB [Dash, 1997] and then be converted to dopamine, making it an effective symptomatic treatment for PD. With long term use of L-dopa, though, some complications arise. The L-dopa has a window of efficiency, if the patient receives too little then no benefit is gained and excess amounts may lead to dyskinesia (involuntary muscle movements). The window of efficiency becomes more restricted with treatment and time, making it harder to find the correct dosage [Olanow et al., 2006], see Figure 2.3. When dyskinesia occurs from a high dose of L-dopa, it is called L-dopa induced dyskinesia.

2.2 DBS and aDBS

Deep brain stimulation (DBS) is an alternative way to treat the motor symptoms of PD. DBS has been used as a treatment for PD since the 1990s [PDF, 2015a]. DBS has shown remarkable potential and has helped alleviate the motor symptoms for many people living with PD. However, the invasive nature of this procedure is its main disadvantage, as a stimulation electrode needs to be surgically implanted deep into the patient's brain. The target for the electrode in humans is in the basal ganglia, usually STN or the globus pallidus interna (GPi, a subsection of globus pallidus) [Kringelbach et al., 2010]. The stimulation protocol used is in open-loop operation, meaning it is programmed by a doctor to a constant stimulation protocol individually adapted to each patient and can only be changed in further meetings with the doctor. This open-loop stimulation type has been shown to reduce the abnormal peak in the beta band mentioned in table 2.1 [Kringelbach et al., 2010]. The

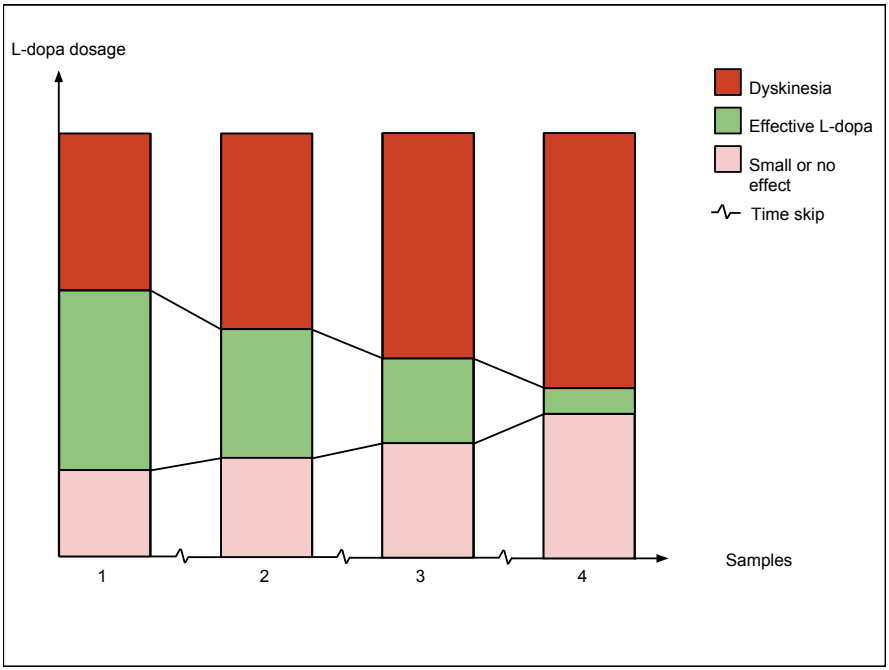

Figure 2.3 Window of effective L-dopa dosage. Showing a theoretical example of four samples taken at different stages of l-dopa treatment. The window for effective l-dopa treatment starts large but gets smaller with time.

next step in DBS research is the adaptive deep brain stimulation (aDBS) that introduces a feedback loop to the DBS which adapts to changes in the signals in the brain. The process of an individually programmed DBS can be quite time consuming and cumbersome. The patient has to frequently travel to a DBS specialist and it can take a number of visits to find the right parameters for the DBS. Conversely, with aDBS the time required for programming after surgery may be reduced since it is adapting itself. There is also hope that the battery life will be extended since the DBS will not be constantly active. The question then arises which signals to record and adapt to, and what to use as a control signal. A review suggests that local field potentials (LFPs) are a good candidate. LFPs are a measure of the electrophysiological signal between two electrodes implanted in the brain and can be seen as the electrical current generated by activation of nearby neurons. LFPs are promising variables with many benefits including [Priori et al., 2013]:

- LFPs correlate with the patient's clinical motor and non-motor state
- LFPs are recordable from the implanted DBS electrode during ongoing DBS

- LFPs are modulated by DBS
- LFPs are still recordable for a long time after DBS electrode implant, and continue to undergo DBS-induced changes over time.

Another possible control variable is the action potential of neurons (spikes) which were successfully used as a control variable in an aDBS that proved to be superior to open loop stimulation in a primate model of PD [Rosin et al., 2011]. A spike is defined as the discharge of energy that occurs when a neuron sends a signal.

Rat model of Parkinson's disease

To be able to study the motor symptoms of PD in a laboratory environment rats can be used as testing animals. To make the rodents display parkinsonian motor symptoms the rats can be lesioned according to the 6-OHDA lesioning protocol [Cenci and Lundblad, 2007]. The lesioning is unilateral, damaging only one half of the brain allowing one half to remain intact. This is very practical when recording LFPs or spikes from implanted electrodes because it is possible to record simultaneously from a healthy side and a parkinsonian side and any changes in activity patterns can also be observed. In the rodent model of PD, there is the same phenomenon as in Figure 2.3, this is sometimes desirable if the experiments aim to study the effects of L-dopa induced dyskinesia which has been correlated to a high increase in the prokinetic oscillations in the motor cortex (80 Hz) [Halje et al., 2012].

2.3 Objectives

The main objectives of this project are to:

- Categorise parkinsonian, L-dopa induced dyskinesia and healthy data.
- Investigate the reticular thalamus as a stimulus target.
- Determine a testing protocol of stimulation.
- Determine a system model for automatic control.
- Design a control scheme for closed-loop stimulation (aDBS) and test it.

Due to the size of the project and time only the first four items are included in this thesis. The last two items of the main objectives aim to merge adaptive deep brain stimulation with the closed-loop automatic control found in robotics, cars, trucks, segways and many other products.

2.4 Limitations

Only one test animal has been used for data recording and the results cannot be stated as a certainty but rather as an observation. Future research should utilise standardised procedures and multiple animals to be able to produce a results with a deeper scientific value.

3

Equipment and Experiments

3.1 Electrode and DBS placement

The recording electrode consisted of an array of 64 channels in the left hemisphere and 64 in the right hemisphere arranged roughly as seen in Figure 3.1. Each one of the brain structures also has a reference channel. The plastic array used for electrode fabrication has extra slots in addition to these 128 recording and 16 reference channels to allow for manufacturing flexibility. The electrodes were formvar-insulated tungsten wires (33 µm) and the reference channels were deinsulated to decrease the impedance. The deep brain stimulation (DBS) electrode was placed in the reticular thalamus (TR) which is part of the basal ganglia.

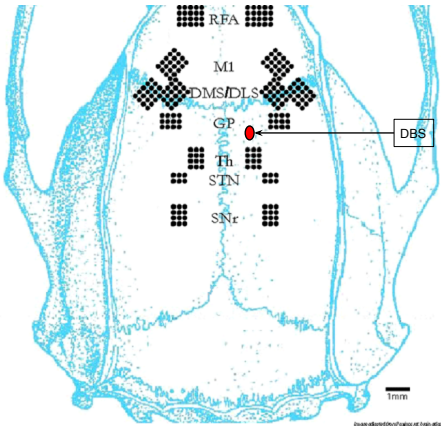

Figure 3.1 The electrode array and placement of DBS electrode in reticular thalamus (TR).

3.2 Data acquisition and stimulus generator

The recordings were done with a data acquisition system composing of:

Equipment	Model
Data acquisition	DigitalLynx10S
Headstages	HS-36
Commutator	PSR-36-4
Headstages → Commutator	TETH-HS-36-Litz
Commutator → Data acquisition	TETH-XTN-xx
Software	Cheetah Software

where the headstages were connected to the electrode through adapters handcrafted at Neuronano Research Center (NRC) and all the components from NeuraLynx Inc. The components responsible of sending stimulus to the DBS electrode were:

Equipment	Model
Stimulus generator	STG4008-16mA
Software	MC_Stimulus II

where the software and stimulus generator were from Multi Channel Systems (MCS) and the whole setup can be seen in Figure 3.2.

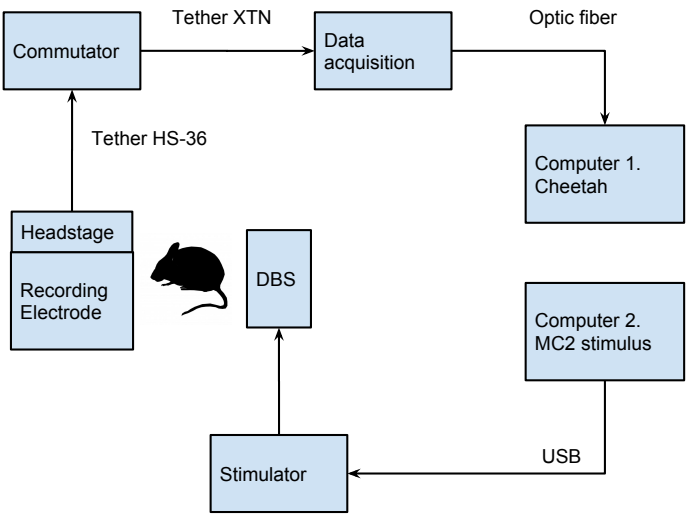

Figure 3.2 The experimental setup for recording and stimulation.

3.3 Stimulation protocol

The different stimulation protocols were programmed in the software MC_Stimulus II [MCS, 2012] provided with the stimulus generator, see Figure 3.3. A stimulation protocol where repeating the stimulation pulse with a 1 Hz frequency was considered a slow enough stimulation for the system to go back to it's natural state between pulses (clinical DBS is usually performed at 130 Hz) and thereby 1 Hz stimulation was also used to gather information about the impulse response. To verify the model two additional frequencies were also used (5 Hz during 30 seconds and 20 Hz for 10 seconds).

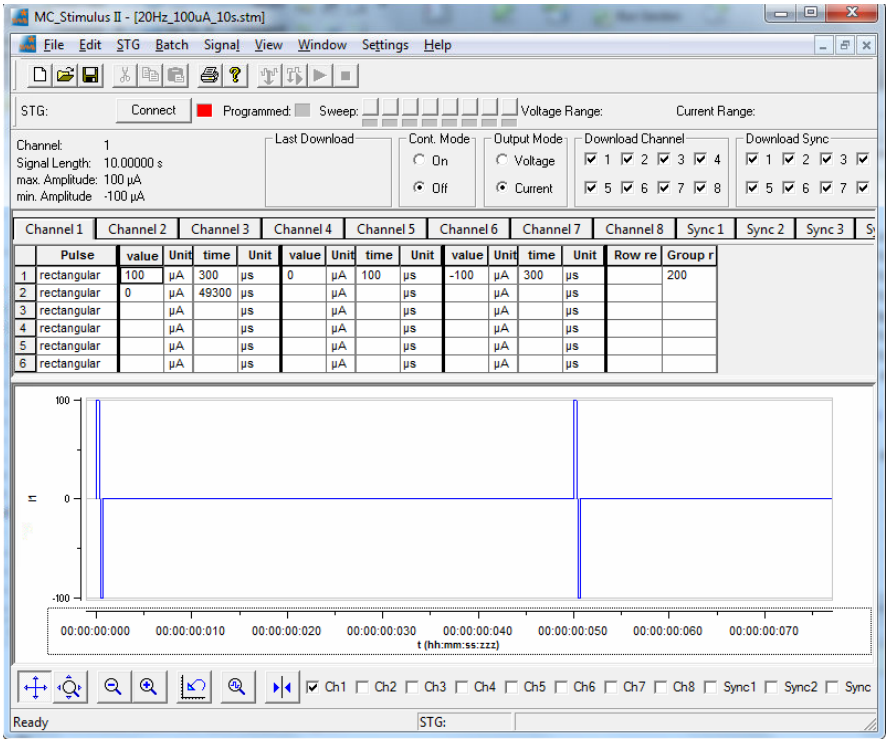

Figure 3.3 The stimulus generation software where the first two pulses of the 20 Hz stimulation during 10 seconds protocol are shown. The pulse is built up by defining height and width three times, then in this protocol it is grouped to a pause, so that two pulses following each other will have 50 *ms* in between. Finally that grouping is repeated 200 times to send 200 pulses during 10 seconds.

3.4 Threshold testing

To find an efficacious amplitude of a pulse, behavioural threshold testing was used. During threshold testing the animal was placed in a open-field environment and then allowed to get familiar with the testing environment for about 15 minutes. The animal's DBS electrode was then connected to the stimulus generator where four different test protocols were tested.

- Low frequency (1 Hz)
- Medium-Low frequency (5 Hz)
- Medium frequency (20 Hz)
- High frequency (100 Hz)

The testing started with the low frequency at a very low pulse amplitude (50 μA). The amplitude was slowly raised until a behavioural reaction from the testing animal was produced. Then the testing was repeated for the rest of the frequencies. After that the animal was given enough L-dopa to produce dyskinesia. The pharmacological effect of L-dopa take some time after injection so there was a waiting period (typically 30 min) until the animal displayed dyskinesia and then new thresholds were measured the same way as before (thresholds during levodopa-induced dyskinesia are usually a bit higher due to the severe motor symptoms displayed).

3.5 Recording data procedure

The animal was put under anesthesia and the recording electrodes were connected to the commutator forwarding the signals to the digital acquisition system according to Figure 3.2. The animal was allowed to move freely in an open-field environment, circular with 1m in diameter, while a baseline was being recorded. The DBS electrode was then connected to the stimulus generator and the stimulation protocols were executed. Between protocols the animal was allowed to rest for a few minutes. The DBS electrode was disconnected and the animal was injected with L-dopa. After the animal had been showing dyskinetic symptoms for 5-10 minutes the DBS electrode was connected to the stimulus generator and the protocols were executed again. The DBS electrode was then disconnected and the animal allowed to rest for 5-10 minutes after which the animal was anaesthetised and the recording electrodes disconnected from the commutator. This process was used to record twice, one with the 1 Hz protocol and one with the 5 and 20 Hz protocol. During the second recording a lot of extra noise was observed during the recording of the parkinsonian state. It was not known why this extra noise was there.

4

Methods

4.1 Signal approximation assumptions

It was necessary to define an impulse that showed efficacious physiological stimulation and delivered as little damage as possible to the brain tissue and the electrode. An article handling this issue presented six different options each with its own advantages and disadvantages [Merrill et al., 2005]. For this project, a charge balanced biphasic pulse with delay was chosen, see Figure 4.1. The pulse is biphasic and thereby has a balanced charge which aids in preventing tissue damage. Without a delay in between the positive and negative part of the pulse seen in Figure 4.1, the pulse may reverse some of the desired physiological effects such as the suppression of spikes (action potentials). Furthermore, if the delay was too long some electrical (faradaic) effects may harm the electrode [Merrill et al., 2005]. The amplitude of the pulse was varied depending on behavioural responses, stimulation frequency and further tests but the pulse width and delay were constant and set to 300 µs and the delay was set to 100 µs making the total length of a pulse 700 µs. This was assumed to be short enough to be characterised as an impulse for control tests and the delay of 100 µs was recommended in the literature [Merrill et al., 2005].

It was assumed that the speed of electricity in the brain tissue is fast enough that a stimulus pulse should generate a stimulus artifact simultaneously in all recorded structures.

4.2 Yield of channels and normalisation

The data were formatted from the NeuraLynx output file into Matlab-friendly files with a script developed at Neuronano Research Center (NRC). The script is a wrapper of the scripts provided by NeuraLynx. Then it was opened in Matlab with a user interface called MeanMachine-Trojan, also developed at NRC. The program was used to get an overview of the recorded LFPs. This program allowed for easy

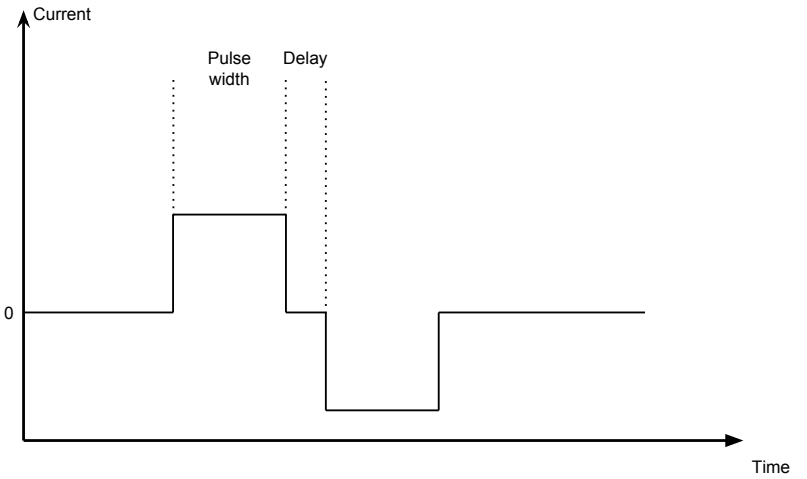

Figure 4.1 A charge balanced biphasic pulse with delay.

navigation through the channels and zooming of scale in time and voltage. It was observed that a lot of the channels were subject to much noise that made their LFP recordings unusable, see Figure 4.2(a) and 4.2(b). The problem was that they were either subject to too much noise and/or being saturated which would interfere with analysis. This noise dominates some channels because their recording electrodes were damaged during the construction of the electrode array. That made them of very high resistance in which case the signal to noise ratio is reduced so that the 50 Hz noise band overpowers the recording signal. All the channels were manually inspected and the unusable ones were marked and removed from further analysis. Then the channels were labelled according to their anatomical location (brain structures and hemisphere). Table 4.1 shows the number of channels and which structures were remaining after this procedure. Signal normalisation was done sep-

Recording 1.	51 of 128 remaining.
Left hemisphere	RFA, M1, DMS/DLS, GP, Thalamus, STN and SNr.
Right hemisphere	DMS/DLS, GP (weak)
Recording 2.	57 of 128 remaining.
Left hemisphere	RFA, M1, DMS/DLS, GP, Thalamus, STN and SNr.
Right hemisphere	RFA, M1, DMS/DLS, SNr

Table 4.1 The channels left in the recordings after cleaning away bad channels. Also states which structures these channels contain.

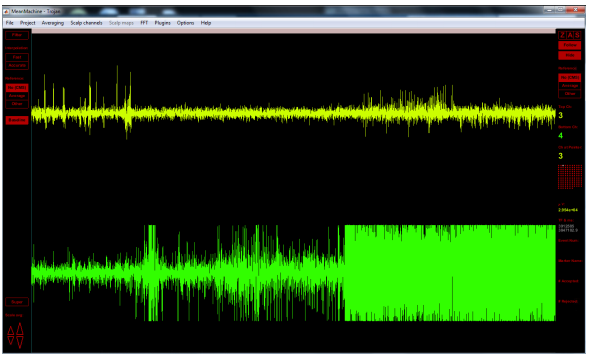

(a)

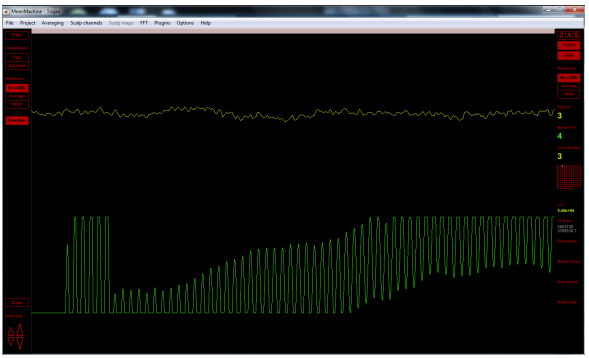

(b)

Figure 4.2 The program MeanMachine which allowed for an easy overview of the recorded LFP. a) Part of the recording. The yellow channel seems to look good while in the green there can be seen a lot of data points where the signal is saturated. b) Zoomed in version of the figure shown in a). Here it is also revealed that the green channel is not only frequently saturated but is also very noisy (50 Hz) while the yellow is clean.

arately for each channel according to Equation 4.1 which centers the data around zero and ranging between -1 and 1. Here x is the channel LFP time series and x_n is the normalised channel data.

$$\begin{aligned} x_1 &= x - \text{mean}(x) \\ x_n &= \frac{x_1}{\max(\text{abs}(x_1))} \end{aligned} \tag{4.1}$$

4.3 Finding time stamps

For further analysis a time stamp of each stimulation pulse was needed in order to create the evoked potentials och PSTHs mentioned below. The time stamp of each pulse was reconstructed offline from the recorded data. To find the time stamps the data were roughly divided into different part: Baseline, 1 Hz stimulus, 5 Hz stimulus and 20 Hz stimulus. Figure 4.3 shows the work flow for each stimulation period to find the time stamps of the stimulation pulses. The local field potential (LFP) data was loaded and normalised. Then, the channels were merged by structure by taking all channels belonging to a structure, summing each time step and then dividing by the number of channels. After this process, there was still no clear indication of where the stimulation took place so the derivative of the data was calculated to identify peaks of sudden increase in the LFPs which proved effective to the purpose of finding groups of values separated from the main bulk and representing the high peaks. The structure derivatives were plotted into histograms, one of which is shown in Figure 4.4. From this information a threshold and structure were found and selected manually. This information was used to find the stimulation pulses time stamps with the help of the function findpeaks in Matlab, which found every peak in the data above the threshold, and with peaks no closer to each other then expected. This was possible thanks to the fact that it was known which stimulus frequency was used. The number of peaks found was compared to the number of pulses sent making sure that no false positives were included. The plot of derivatives was also manually inspected for this purpose. The threshold was manually adjusted until at least 80% of the sent pulses were found while still not allowing any false positives. The identified time stamps were extracted from the derivative of the structure data, which means that it is most likely to be after the delay in the biphasic pulse see Figure 4.1. Time stamps were shifted two or three samples, depending on manually identifying the onset of the stimulus peak, to take this time shift into account, and were plotted with the non-derivative of the data. Still, some of the time stamps were not in synchronisation and needed to be adjusted. This was done with the help of cross-correlation. First a time stamp was manually identified that appeared to be accurate. This was used to make a template with n values forward and backward depending on the stimulus frequency (short enough to not encounter the next or previous pulse). Then all time stamps were looped through and each was made into a data set in the same way the template was made. Then cross-correlation (with the xcorr function in Matlab) was used to find at which timelag the data set best fitted the template. The time stamps were then moved accordingly. The time stamps were finally manually inspected, one by one, plotted together with the LFP data to confirm their validity. In the future, it would be recommended to record the time stamps instead of going through this process, both for better accuracy and for a smoother work flow.

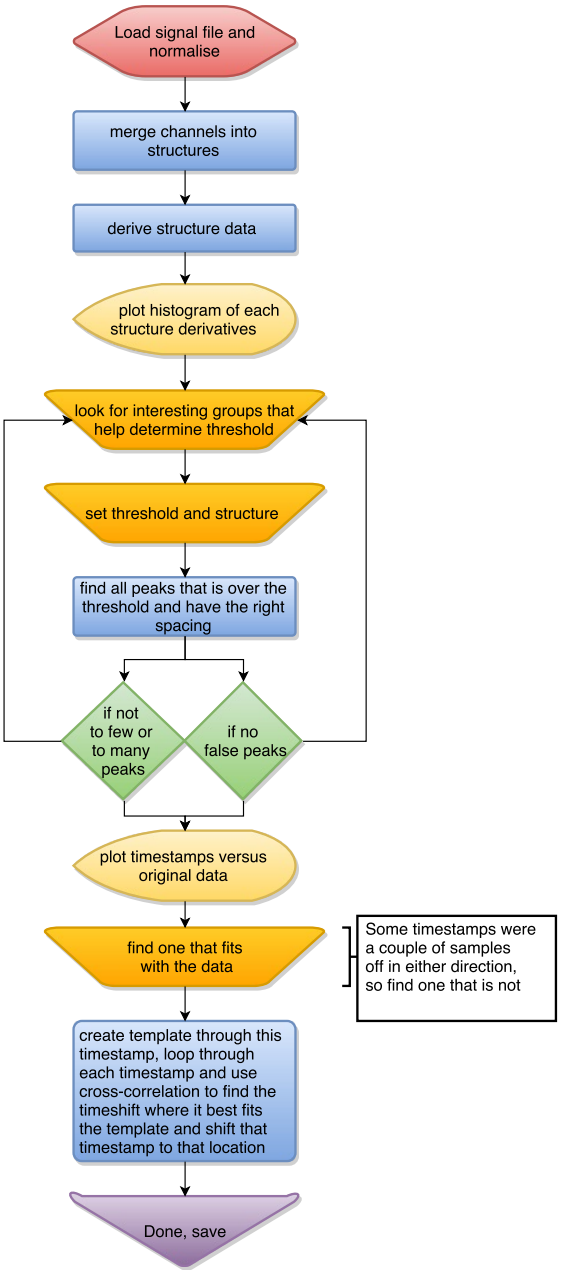

Figure 4.3 The workflow of the script that calculates the time stamps.

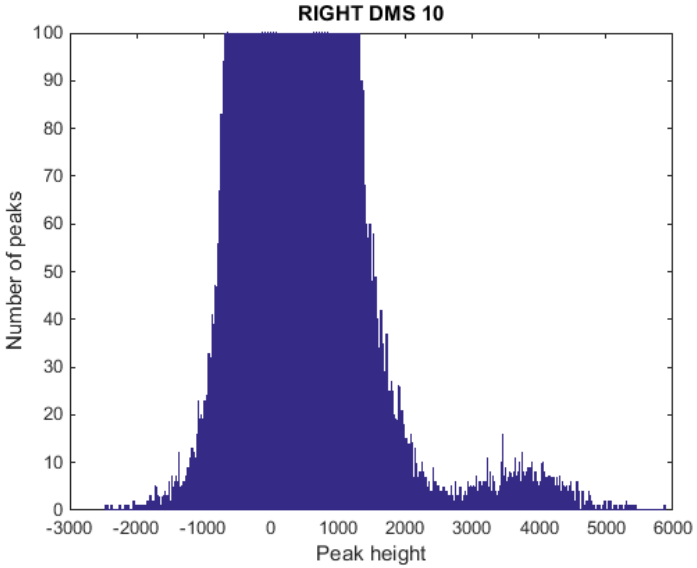

Figure 4.4 A histogram of the peaks found in the derivative of the normalised local field potentials in the right DMS (dorsal medial striatum, right hemisphere (lesioned)). A group can be seen that differs from the norm and the onset of that group will be used as a basis for the finding of a threshold for the identification of the time stamps.

4.4 Evoked potentials

The evoked potential is the electrical potential that can be measured in the neuronal tissue as a physiological response to a stimulus. In this case, the evoked potential would be the response of the neurons in the vicinity of the recording electrode following an electrical stimulus pulse. The mean of the evoked potentials were calculated with the help of the MeanMachine software by loading the extracted time stamps and then for each channel calculating the mean response defined by a number of pre-samples and post-samples around the time stamps. Data sets were separated according to the applied stimulation frequency see Table 4.2.

Stimulation	Pre-samples	Post-samples
1 Hz	100	900
5 Hz	50	150
20 Hz	12	38

Table 4.2 The number of samples before and after the time stamp of the stimulus pulse included in the evoked potentials for the different stimulation frequencies. The sample frequency rate was set to 1017 samples per second.

Field Power

Among the recorded channels some are physically very close and the 33 µm tungsten wires are flexible and might bend towards each other during implantation. There is also the possibility that a channel is almost the same as another but with a different sign depending on which reference channel was used. In order to merge all channels per brain structure a standardised field power was used. First the standard deviation across all channels in a structure were calculated, see Equation 4.2, where x_i is channel *i*s LFP time series data, $\langle \mathbf{x}(t) \rangle$ is the average across channels at that timepoint and N is the number of channels in the structure.

$$s(t) = \sqrt{\sum_{i=1}^{N} \frac{(x_i(t) - \langle \mathbf{x}(t) \rangle)^2}{N}} \tag{4.2}$$

Then it was normalised to the standard deviation of the baseline.

$$s_n(t) = \frac{s(t)}{\mathrm{std}(\mathbf{s}_{base})} \tag{4.3}$$

The baseline, $\mathbf{s}_{base}$, was defined as the samples before the stimulation pulse according to Table 4.2.

4.5 Peristimulus time histogram

A peristimulus time histogram (PSTH) is a commonly used in neurophysiology and is a time histogram over neurons action potentials (spikes) in response to an event which here is an electrical stimulation pulse. As a first step, the spike data needed to be processed to find what parts of the data were neurons firing and to separate those data from stimulus artifacts or noise.

Extraction of spike data

This section will explain how the action potentials were found and separated from artifacts/noise. For the PSTH the 1 Hz data were used, using the time before the injection of L-dopa. First the active neurons from each channel, there could be multiple per channel, needed to be identified and separated in a process referred to as spike sorting. The sorting was done with the help of a program called ZippySort which is a program written by NRC and based on methods by [Fee et al., 1996]. The raw data were loaded into the program and then each channel was manually inspected in the search for clusters representing separate neurons. The ZippySort graphical user interface (GUI) can be seen in Figure 4.5 and 4.6. ZippySort takes out the first 10000 recorded spikes from the channel and creates the summary window, feature window and aggregation tree. Some clusters might have been an active neuron but had just too few spikes to tell so they were excluded. The aggregation tree in Figure 4.6(c) were used to split large clusters into smaller which sometimes revealed neurons with good waveforms hidden in larger clusters. The tree was also used when two clusters were very close with a very similar looking waveform to merge them, which sometimes revealed that they represented the same neuron.

A good cluster representing a neuron was determined to have these properties:

- A clear waveform.
- None or few interspike intervals (ISI) under the red dotted line (1.6 ms).
- A clear grouping in the feature windows principal component analysis (PCA). A prime example of a clear grouping would be a circular shape of the cluster and the closer the middle of the cluster the tighter the groupings.

An example of a cluster that fulfilled all those qualities is Cluster 7, see waveform in Figure 4.5(b) and clustering marked green in Figure 4.6(a). After all the channels had been processed this way, the spike data from neurons were extracted and saved. The same process was repeated but instead looking for artifacts where an artifact was determined to have these qualities:

- Unnatural waveform, for example saturated signals.
- ISI almost always under the 1.6 ms mark.

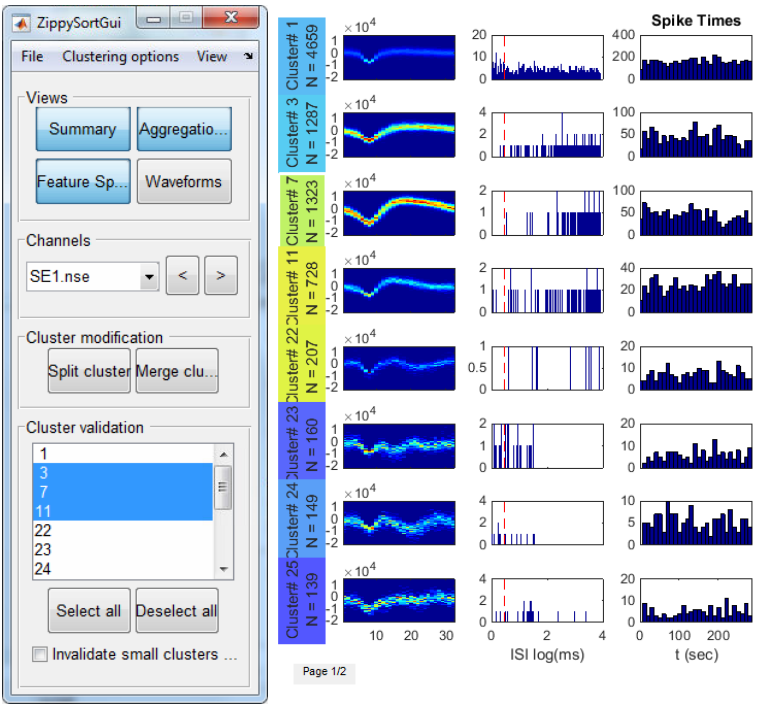

Figure 4.5 ZippySort. a) The GUI where the plots shown were chosen and the promising clusters selected for saving. b) The Summary window. Showing the waveform, inter spike interval (ISI) and spike times.

- An odd looking group in the PCA. Often the artifact cluster would take the form of a line or very tight cluster instead of a natural spread.

PSTH

Histograms were plotted from 100 ms before the onset of the stimulation pulse to 900 ms after it. The number of events found through the time stamps identification script was N = 952 for the parkinsonian state and N = 1000 for the dyskinetic state. From all of the events the spikes from each event window (-100 ms to 900 ms of time stamp) were extracted and split into 1 ms bins. This was done for all the found neurons with the help of a Matlab function called getPeriEventResponse developed at NRC. The responses were grouped into their respective brain structures and plotted. To clearly see behaviour that differed from the normal one, the Z value of the histograms were calculated and their respective values presented as power over time

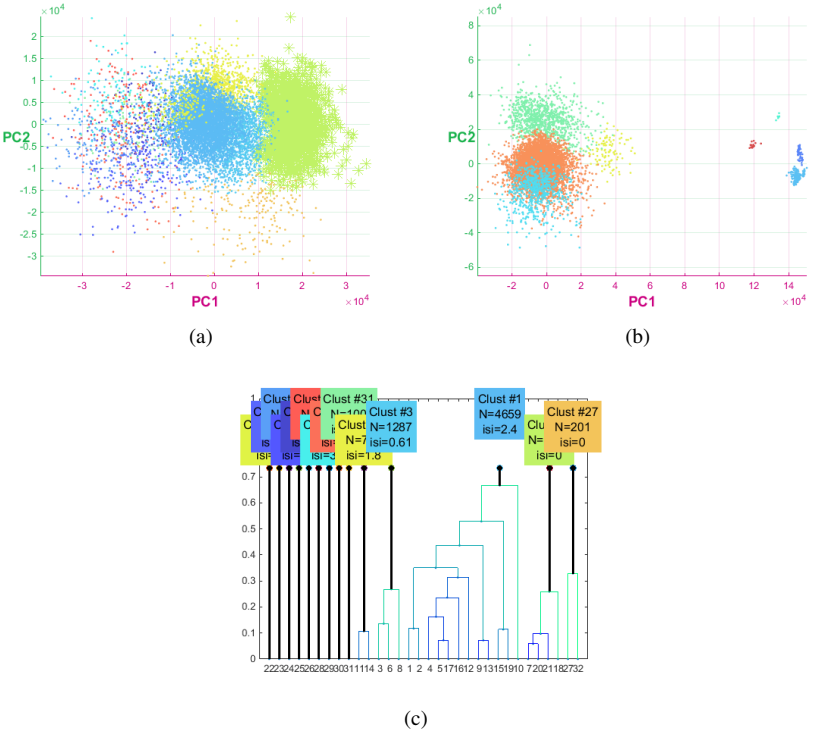

Figure 4.6 ZippySort. Feature window (a and b) and the aggregation tree window (c) a) The cluster marked with + (light green) is an example of a possible good neuron and is Cluster 7 from Figure 4.5(b) while in b) small tight groups can be seen to the right of the main groupings, these are likely artifacts/noise. c) Shows detected subgroups that might be neurons and allows for splitting and merging clusters.

diagrams. A Z value is a statistical method that shows the signed number of standard deviations the data set is from the mean. When stimulating a stimulation artifact is expected, to see how the artifact affected the PSTH the artifact neurons were used in the same way to plot the artifact PSTH seen in Figure 4.7, here it was considered sufficient to look at the PSTH.

4.6 Spectral Analysis

Power spectral density diagram

The power spectral density diagrams (PSDs) were created from the LFP data from recording 2. The data were split into a baseline period, where there was no stimula-

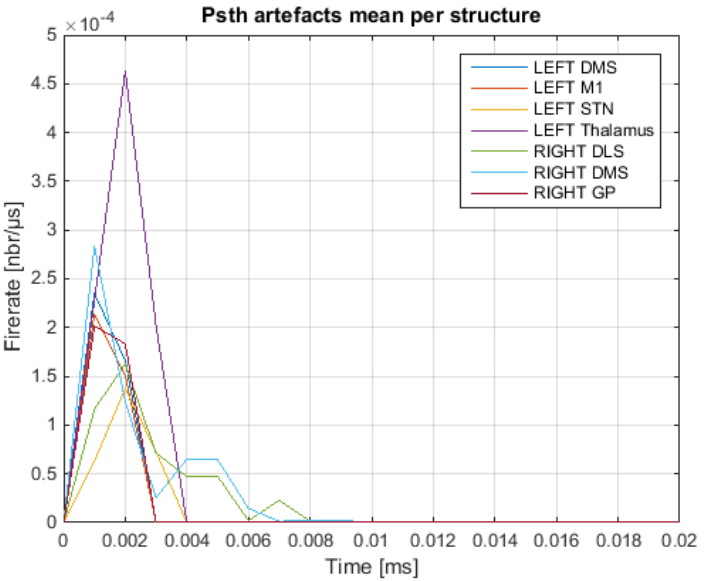

Figure 4.7 A PSTH over the stimulation artifact and or noise from recording 1. The spikes from the found neurons were grouped into brain structures. Not as many structures were found as for the data that were identified as neurons.

tion, and all data recorded after L-dopa injection (including stimulation). The data were first normalised as described in Section 4.2 and merged into the channels of the brain structures. Then the power spectrum was calculated with an NRC developed function called getAutoSpectrumLight. This function uses a multitaper method to estimate the power spectra. Multitaper is a spectral density estimation technique that reduce estimator bias by taking multiple independent estimates of each sample and then averaging the results. The multitaper was set to window length of 6000 samples and an effective frequency resolution of 0.678 Hz. The spectrogram for the L-dopa data was plotted and clear stimulation periods was seen (see Figure 4.8) and the times of these periods were noted. To not allow the artifacts from the stimulation or the stimulation frequency itself to affect the PSD, all power values within the noted periods were set to zero. The power values were then summed over the time axis creating the power vector of the PSD. The channels were then merged into their respective brain structures, this revealed that the data contained pink noise (noise that trends similar to a linear decrease in a log-log diagram). The pink noise was reduced with a NRC developed function called convert_to_dBpink. In this pink noise reduction the data gets adapted to frequency ranges. These ranges are the frequencies where clear a pink noise trend could be seen in the PSD see Figure 4.9, the output of the function can be viewed as a measurement of signal to noise ratio

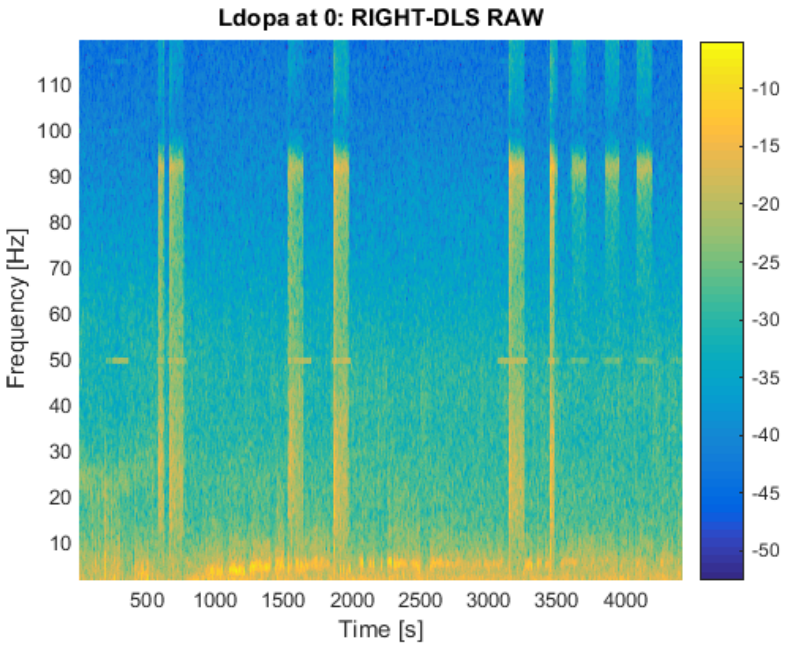

Figure 4.8 A spectrogram from the time of L-dopa injection to the end of the recording. Showing clear stimulation artifacts at multiple times where almost the whole frequency spectra is increased in power.

expressed in pink decibels.

4.7 System Identification

Automatic control is commonly used to regulate the movement of machines or robots. A regulator is created and adapted to each machine's purpose to quickly, accurately and safely move from point A to point B. To be able to add a controller to a system it is necessary to understand its dynamics and that different systems have different levels of complexity. Sometimes the system dynamics can not be deduced from theory, in which case the system dynamics need to be identified from the measurements before the automatic control theory can be applied. Through observation of how the system reacts to input and with the use of clever algorithms, a model of the system can in many cases be identified. A typical way to describe a system or controller is by means of the transfer functions. The transfer function can be deduced from the state-space equations of a system which classically (in discrete

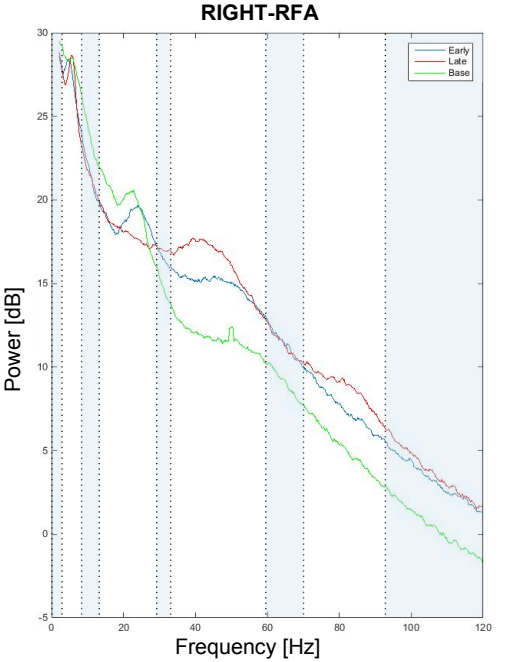

Figure 4.9 An example of a power spectral density diagram with pink noise. The data were obtained from the RFA structure during recording 2 and show the frequencies before injection of L-dopa (GREEN), from injection of L-dopa to about 30 minutes after L-dopa injection (BLUE) and the rest of the recording (RED). Here it is shown how the frequency ranges (light blue areas) used for pink noise reduction was found, which are all frequency ranges without notable peaks.

form) looks like Equation 4.4 and 4.5.

$$x_{k+1} = Ax_k + Bu_k + v_k \tag{4.4}$$

$$y_k = Cx_k + Du_k + e_k \tag{4.5}$$

Here x_k is a vector that contains the current values of the state variables, y_k is the output(s), u_k the control inputs to the system, v_k and e_k are disturbances from outer sources or modelling errors. The matrices A, B, C and D determine the dynamics of the system. The transfer function is the z-transform of how the input is transformed into the output and can be calculated through the A, B, C and D matrices according to Equation 4.6 where H is the discrete-time transfer function.

$$\frac{Y(z)}{U(z)} = H(z) = C(zI - A)^{-1}B + D \tag{4.6}$$

Markov parameter realisation

The algorithm used for finding the state-space equations was the Markov parameter realisation. Markov parameter realisation is an algorithm that identifies the A, B and C matrices from impulse response data and was introduced by Ho and Kalman [1966] and later modified by Kung [Johansson, 2012]. The algorithm starts by looking at multivariable transfer function

$$H(z) = \sum_{k=0}^{\infty} H_k z^{-k}$$

where H_k is the Markov parameters and $H_k \in \mathbb{R}^{p \times m}$. It is assumed that the initial state is zero ($x_0 = 0$) . The algorithm handles the problem of finding the three matrices A, B and C from

$$H_k = CA^{k-1}B \qquad\qquad k = 0, 1, 2, 3, ..., N.$$

Each H_k is a $p \times m$ time sample of the impulse response where p is the number of outputs and m is the number of inputs. In this master thesis only the case of $p = 1$ will be handled which means that each time sample of H_k will directly be the time samples of the impulse response in each output. To find the three matrices the Markov parameters were organised into a Hankel matrix using suitable numbers for r and s

$$\mathscr{H}_{rs}^{(k)} = \begin{pmatrix} H_{k+1} & H_{k+2} & \cdots & H_{k+s} \\ H_{k+2} & H_{k+3} & \cdots & H_{k+s+1} \\ \vdots & \vdots & \ddots & \vdots \\ H_{k+r} & H_{k+r+1} & \cdots & H_{k+r+s-1} \end{pmatrix}$$

From the Hankel matrix the singular value decomposition can be computed

$$\mathscr{H}_{rs}^{(0)} = U \Sigma V^T$$

and after the system order n is determined by investigating the Σ matrix the singular value decomposition matrices will be adapted to it by taking the first n diagonal values from Σ, the n first columns of U and the first n columns of V into Σ_n,U_n and V_n. The A, B and C matrices can then be deduced from the following equations [Johansson, 2012]

$$\begin{aligned} A_n &= \Sigma_n^{-1/2} U_n^T \mathscr{H}_{rs}^{(1)} V_n \Sigma_n^{-1/2} \\ B_n &= \Sigma_n^{1/2} V_n^T E_u \\ C_n &= E_y^T U_n \Sigma_n^{1/2} \\ D &= H_0 \end{aligned}$$

where E_y and E_u are defined as the selector matrices

$$E_y = [\mathbf{I}_{p\times p} 0_{p\times(r-1)p}]^T, \qquad E_u = [\mathbf{I}_{m\times m} 0_{m\times(s-1)m}]^T.$$

In this thesis the algorithm uses the impulse response from the system which here is defined as the evoked potential. The evoked potentials from the 1 Hz, 5 Hz and 20 Hz stimulation was each tried out separately with the algorithm. The samples before the stimulation point and the five samples after that, which was seen as the artifact period revealed by the artifact PSTHs, was removed since in this thesis, the interest lies in modelling the natural response, not the stimulation artifact. Then a Matlab script called impulseresponse.m written by Rolf Johansson was used to calculate the A, B, and C from the impulse response according to the Markov parameter realisation algorithm described above. The order of the system was determined by looking at the single value matrix values, an example of this can bee seen in Figure 4.10. In this example the lines meet roughly around 10 which would then be chosen as the estimated system order. This was done separately for the left (healthy) and

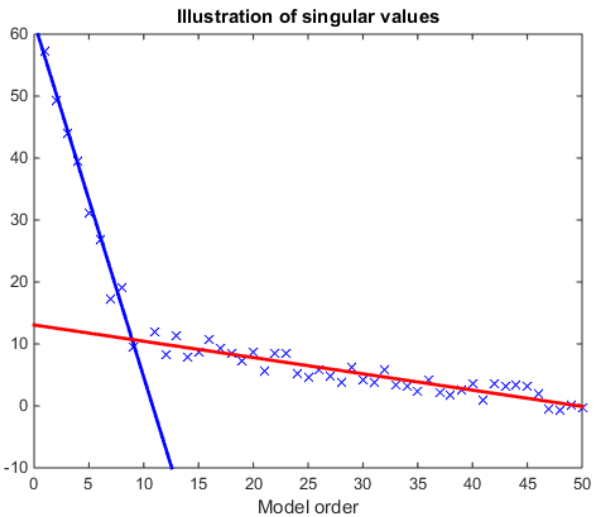

Figure 4.10 An example of how the singular values from the Σ matrix from the singular value decomposition could look. The intersection of the lines would be used to find the order of the system, the blue can be seen as valid system variables and the red as noise or other disturbances that should be excluded from the model.

right (lesioned) hemispheres for the 1 Hz, 5 Hz and 20 Hz evoked potentials. From these matrices discrete system transfer functions were created with the ss function provided with the Control Systems Toolbox in Matlab.

4.8 Validation of model

The discrete-time state-space models were used in the simulation of stimulation pulses incoming with a frequency of 1, 5 and 20 Hz. These data were saved and used to find the simulated evoked potentials. This was done not through Mean-Machine but by simulating the 1, 5 and 20 Hz stimulation to the system with the lsim function from the Control System Toolbox in Matlab. Then going through the simulated data and calculating the mean response around the time stamps of the simulated impulses that were created with the simulation input data. The channels that were the same in recordings 1 and 2 were extracted, the simulated and recorded responses were plotted together with the error between them in each time point. This was done with both of the reference data sets 5 and 20 Hz. This revealed that the model created from the 1 Hz evoked potentials had difficulties recreating the 5 Hz and 20 Hz responses accurately. A model was thus also created for the 5 and 20 Hz response of which the 5 Hz had the appearance of also returning to a resting state between pulses while the 20 Hz did not. The 5 and 20 Hz response models were created the same way that the 1 Hz response model and the complexity of the models compared. A Bode diagram was created from all three models containing all the channels corresponding to the right hemisphere and the DLS structure. The magnitude part of the Bode diagram was compared to the PSD of the DLS structure in the right hemisphere. The results are presented in the next chapter.

5

Results

5.1 Threshold testing and observations of visual behaviour

The responses to different stimulation frequencies can be seen in Table 5.1. Clear visual responses could be seen before the injection of L-dopa. After the L-dopa induced dyskinesia set in, no behavioural responses could be seen due to the severity of the motor symptoms. Testing was done up till 1.3 times the threshold level seen before injection of L-dopa.

Stimulus	Reaction
1 Hz	No visual responses.
5 Hz	The rat turned a bit and sniffed.
20 Hz	Turned head contra lateral to lesioned hemisphere.
100 Hz	Strong reaction.
	Turned axially and twitching observed in paw.

Table 5.1 The responses seen in the rat during threshold testing when the rat was in a parkinsonian state.

5.2 Power density spectra of LFPs

In the pink noise reduced power density spectra seen in Figures 5.1 and 5.2, clear indications of parkinsonian related oscillations can be seen. The left hemisphere was left intact and was used as a reference to normal while the right side was subject to 6-OHDA lesions. In the lesioned (right) hemisphere peaks are evident in the 20 Hz range during the baseline (before L-dopa injection) and these vanish as the L-dopa starts affecting the brain. These oscillations have previously been connected to antikinetic parkinsonian symptoms [Kringelbach et al., 2010] and in contrast the control hemisphere (left) was left largely unaffected with no peaks visual in the 20

Hz range. In the 35-50 Hz range a broad band increase in the lesioned hemisphere was observed from the baseline to the later time period where the L-dopa is in full effect, this bringing it up to something comparable to the control hemisphere which was moderately affected by the L-dopa injection. The other clear difference is the 80 Hz peak seen in the lesioned hemisphere in the later stage L-dopa where clear dyskinesia was observed. These 80 Hz oscillations were claimed to be strongly associated with the observed L-dopa induced dyskinesia by [Halje et al., 2012]. A 50 Hz power line disturbance is also observed.

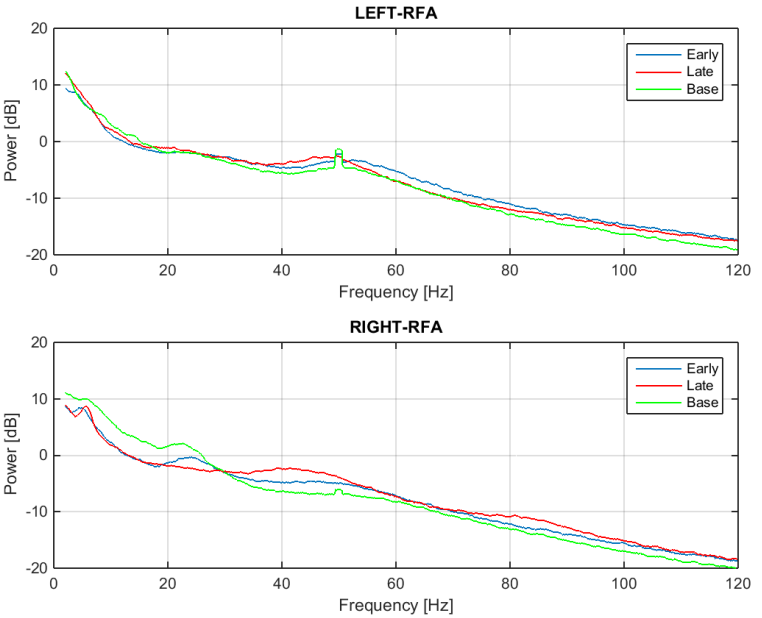

Figure 5.1 Power density spectra of the cortex region called rostral forelimb area (RFA) of both hemispheres. The GREEN (Base) plots are from the baseline of the recording. The BLUE (Early) is from the first 2000 seconds after L-dopa injection. The RED (Late) is the rest of the recording. The data used are from recording 2 and all the sections containing stimulation were set to zero before calculation of the PSD, the data show a clear pink noise trend.

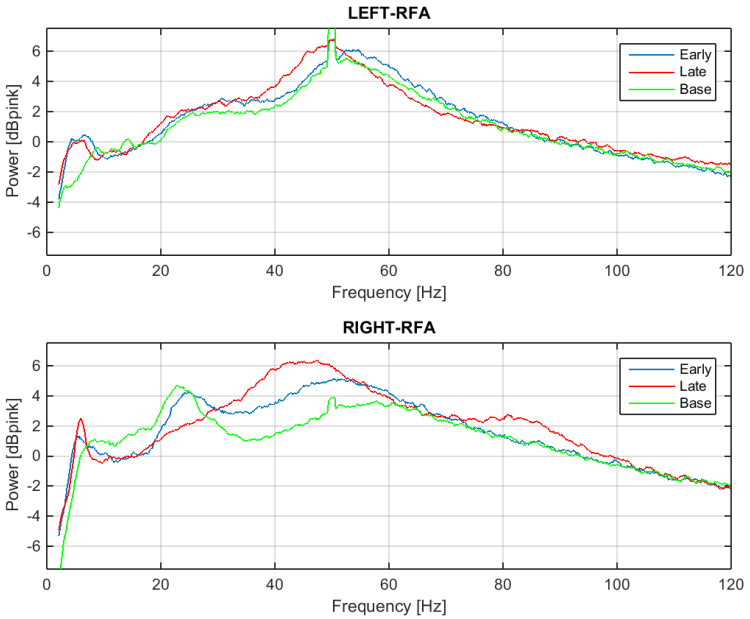

Figure 5.2 The same data set as in Figure 5.1. Here the data are instead presented in pink noise decibels revealing narrow band oscillations more clearly than before. A 50 Hz power line disturbance is observed.

5.3 Evoked potentials

The evoked potentials from 1 Hz stimulation can be seen in Figure 5.3. In the figure, a clear split can be seen around the 100 ms mark where some channels are positive and some negative. As explained in the method chapter this can cause some problems.

Field power

The field power from the evoked potentials can be seen in Figure 5.4 where the 1 Hz stimulation response is compared in parkinsonian and dyskinetic states and Figure 5.5 where the 1, 5 and 20 Hz stimulation responses are compared in the dyskinetic state. The responses of comparable structures in Figure 5.4 have a lot of similarities but also differences. In the dyskinetic state the field powers are decreased and some of the post-stimulus oscillations were reduced compared to the parkinsonian state. During higher frequency stimulation the field power decreased even more and the evoked potentials were quicker to return to a resting state. The

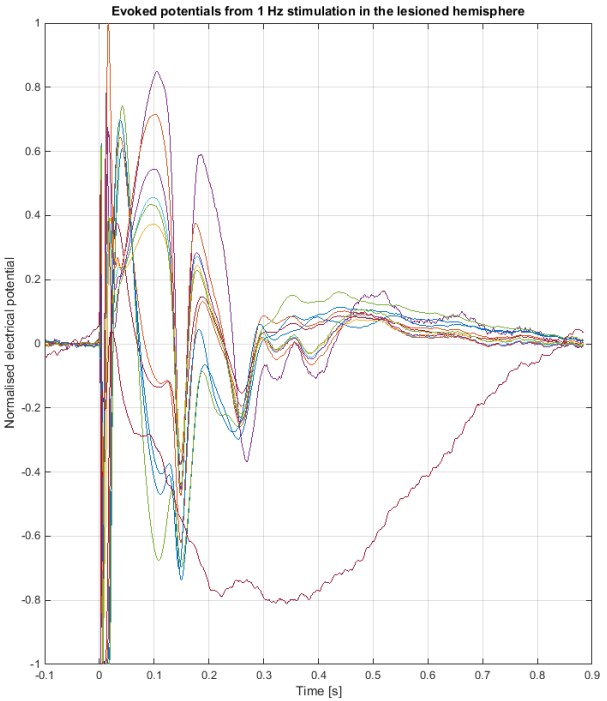

Figure 5.3 Evoked potentials in the lesioned hemisphere. Evoked from 1 Hz stimulation during a parkinsonian state. During the first milliseconds there is an artifact during the stimulation pulse. Then the evoked potential can be seen as an oscillatory pattern. Around 100 ms there can be seen a clear split where some of the channels show positive and some negative sign. One of the channel responses do not follow the others and was therefore removed before applying the Markov realisation algorithm.

dorsal medial striatum (DMS) responses between the different stimulation protocols had little in common except for a small oscillatory pattern. There are hints of peaks at 20 ms and 45-50 ms that could be parts of the big effects seen in 1 Hz stimulus but that is unclear. Between the 5 Hz and 20 Hz responses the field powers have decreased again and also the shape of the signals are different, except for the artifact peak and one or two peaks that behave the same in both responses (such as substantia nigra pars reticulata (SNr) at 18 ms). The responses seen in the field potentials display a change in behaviour when applying different stimulus protocols. It is evident from the field potentials that at higher frequencies inhibition becomes more prominent.

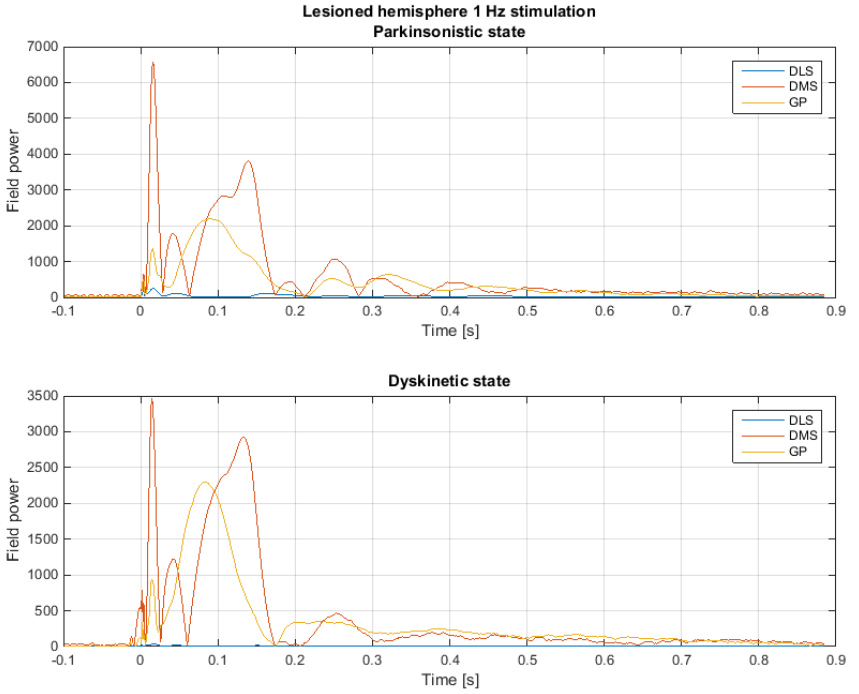

Figure 5.4 The field powers that are evoked from 1 Hz stimulation in parkinsonian and dyskinetic state. On the x axis is time in seconds and on the y axis is the field power. Time t=0 is the onset of the stimulus. During the parkinsonian state the field power is generally higher in the DMS while they stay about the same in globus pallidus (GP). Both DMS and GP have similar properties in both states but some peaks are missing or only hinted at in the dyskinetic state which is clearly seen after 200 ms.

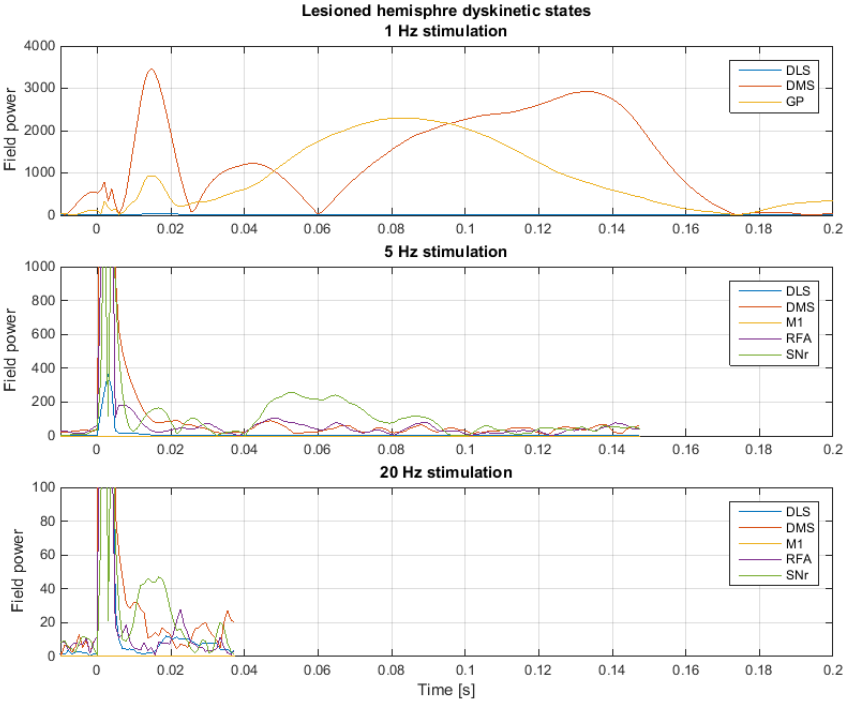

Figure 5.5 The field power evoked from 1, 5 and 20 Hz stimulation during the dyskinetic state for the time period -10 to 200 ms where 0 is the onset of the stimulus. There are clear differences between the field power created from 1 Hz stimulus and the 5 and 20 Hz. The field power decreases with higher frequency and similarities between DMS in all cases are few. The 5 Hz and 20 Hz responses may be more closely related, at least there is a peak in the SNr in both around 18 ms.

5.4 PSTH of evoked action potentials

The peristimulus time histograms (PSTHs) are displayed as power plots of the Z-scores in Figure 5.6. Reoccurring peaks of activity can be seen as a response to a stimulation pulse. The artifacts identified in Figure 4.7 showed that most artifacts died out at 5-8 ms and therefore the peaks earlier than 8 ms were deemed to be untrusted. A point of interest is the left thalamus which is contralateral to the DBS electrode and is the only structure that responds to the stimulation by being completely silenced for one or two milliseconds. Over the whole basal ganglia, both hemispheres, 5-10 Hz oscillatory activity is observed for ca 450 ms in the parkinsonian state. The left thalamus is the only structure showing a significant inhibition (Z-score of -2 or lower) between the first two activity peaks (40-100 ms) in the parkinsonian state. Globus pallidus (GP) is seen to be around -1.8 for the same duration. The dyskinetic state differs a bit showing a stronger inhibition in the subthalamic nucleus (STN), also of significant strength. The dyskinetic state shows different behaviour where it follows the parkinsonian response up to ca 200 ms and afterwards no extra peaks or valleys of activity stick out from the ordinary with the oscillations seen in the parkinsonian state gone.

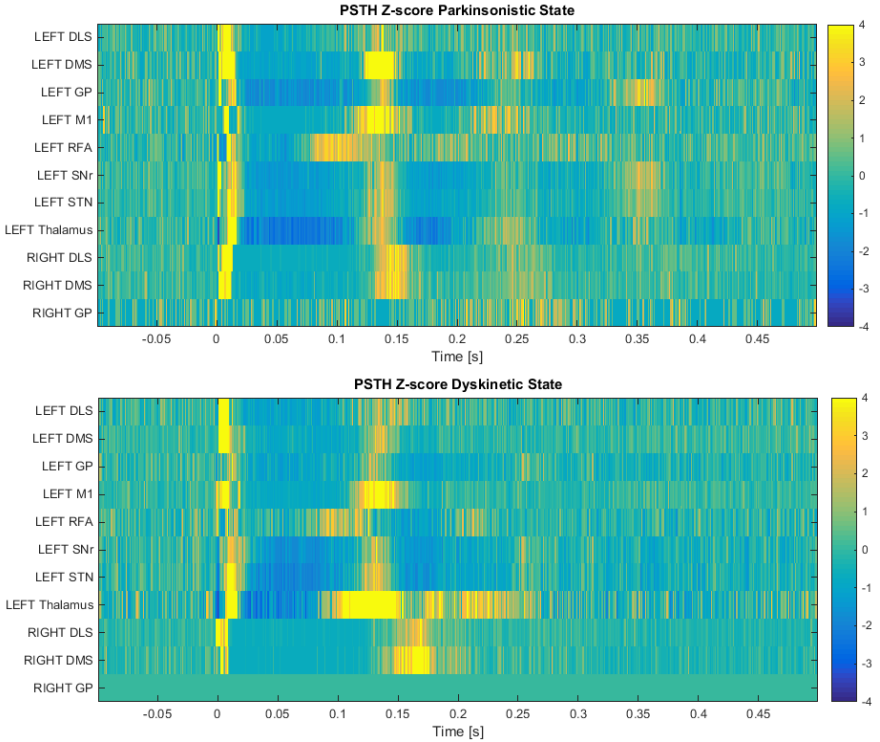

Figure 5.6 The PSTH plotted as a powerplot of Z-scores. The max value of Z-score should be considered to be 4+ since close to the artifact values of 50-100 was observed. Around 100-130 ms the activity also produced a Z-score of around 30 in most structures.

5.5 Markov realisation model responses

In Figures 5.7, 5.8 and 5.9 the recorded evoked potentials are presented together with the simulated responses from the model corresponding to each figure's stimulation protocol and the error between them. The order required in the model was defined from the singular values from the Σ matrix from the singular value decomposition shown in Figure 5.10. The orders for the models were determined to:

Stimulation protocol	model order
1 Hz	20
5 Hz	10
20 Hz	5

Both the system models created from 1 and 5 Hz evoked potentials produce a simulated response with an acceptable error, the 20 Hz system model however, does not. The Bode diagrams for the right hemisphere and the DLS from the system models are seen together with a PSD if the same location in Figures 5.11 b) and 5.12. This was studied to see if some of the Bode diagrams showed a gain in frequency areas where the PSD plot showed peaks. Some similarities can be found, in both the 1 Hz and 5 Hz system models a peak can be seen around 6 Hz and a decrease in magnitude directly after that which can be seen in the PSD. In the magnitude Bode diagram from the 5 Hz there is also the trend of a rise in magnitude around 30-80 Hz and thereafter slowly decay which is also seen in the PSD. Other than those similarities in shape, the diagrams are mostly different. The system model based on 1 Hz evoked potentials shows mostly a positive gain until 100 Hz and the system model based on 5 Hz evoked potentials displays suppression over almost all frequencies except for one channel in which there is a positive gain over the 20-100 Hz frequencies.

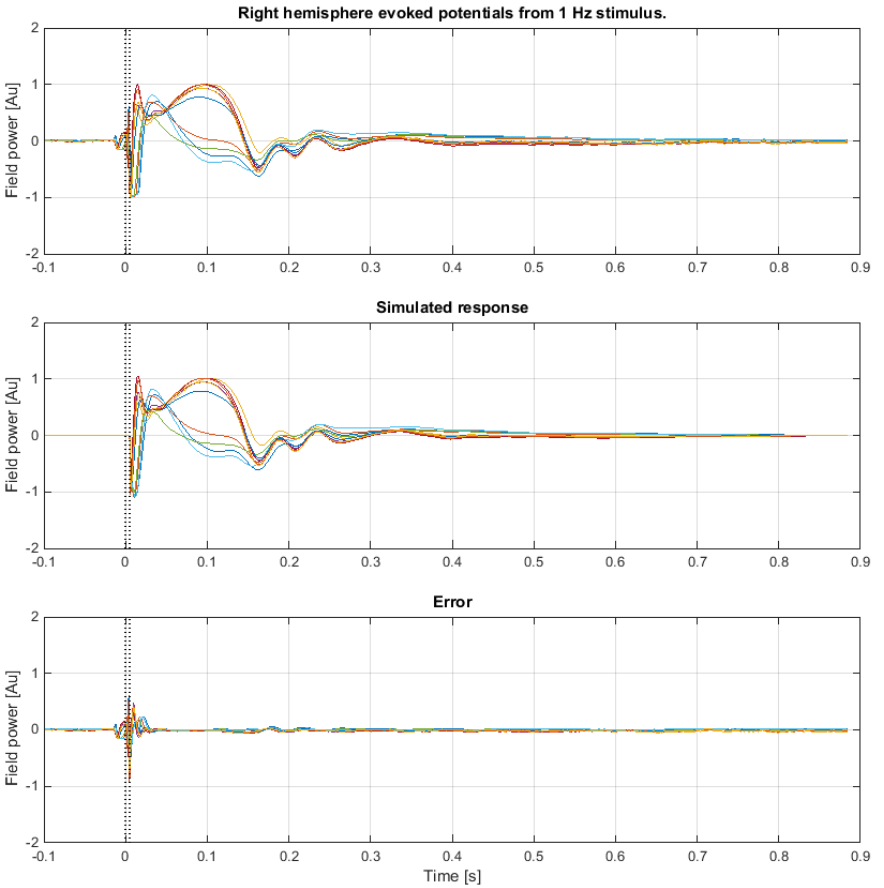

Figure 5.7 Evoked recorded vs simulated. 1 Hz. The dotted lines represent the time interval of stimulation artifacts. The simulated responses were built from a system model of order 20 created from the evoked potentials from 1 Hz stimulation.

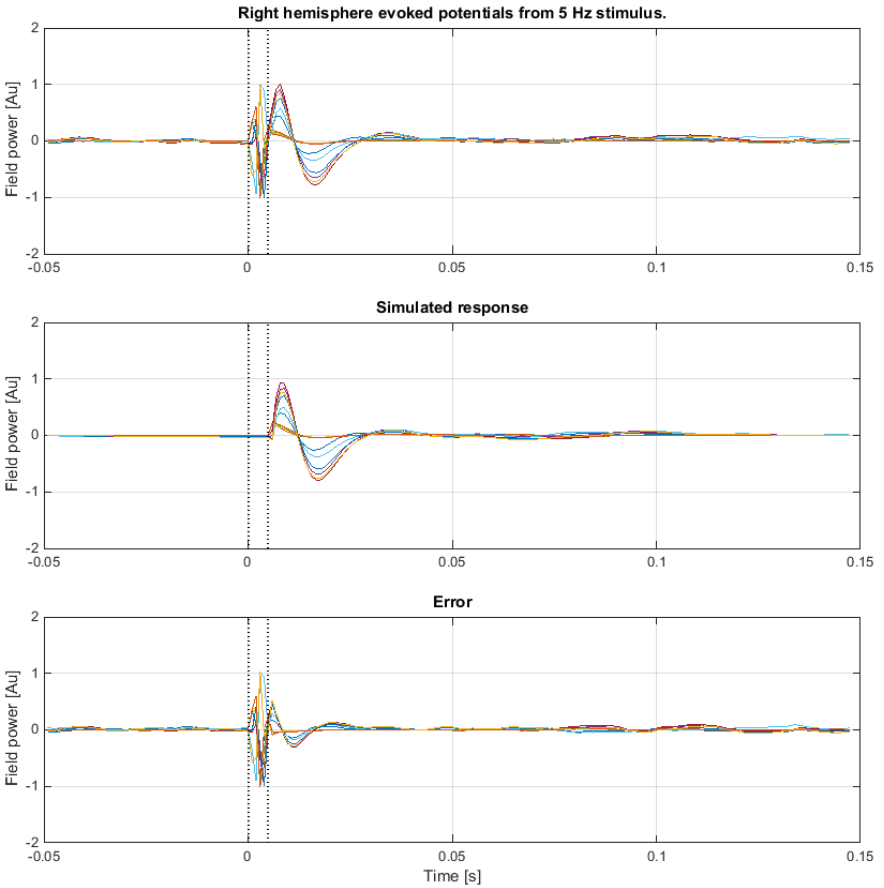

Figure 5.8 Evoked recorded vs simulated. 5 Hz. The dotted lines represent the time interval of stimulation artifacts. The simulated responses were built from a system model of order 10 created from the evoked potentials from 5 Hz stimulation.

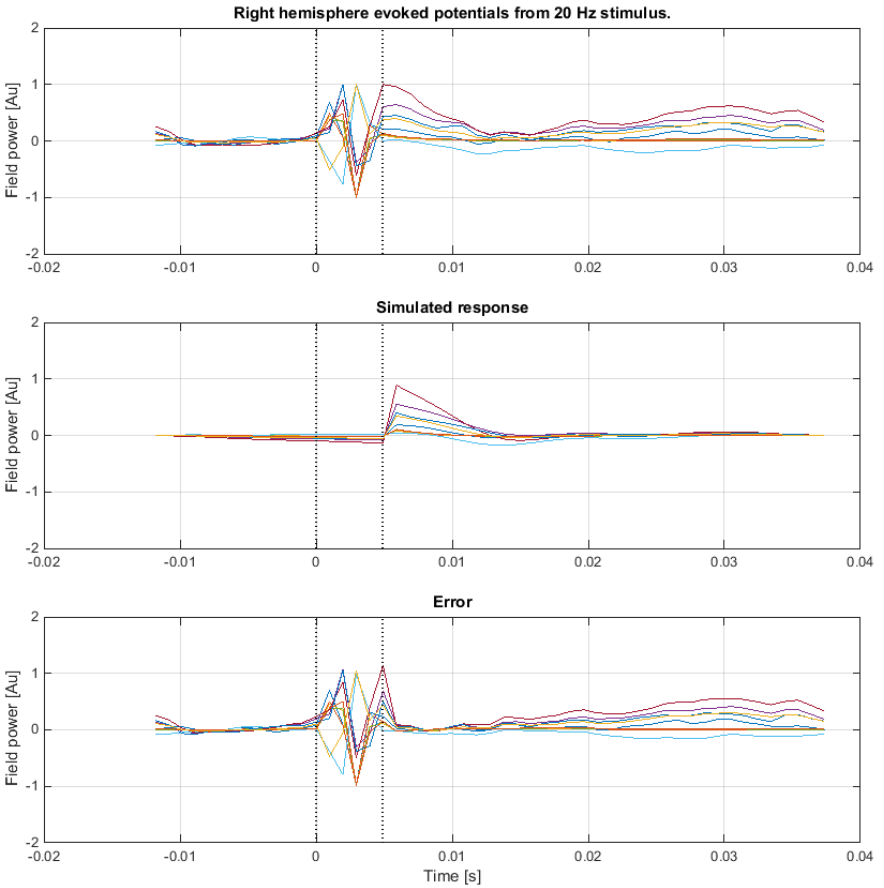

Figure 5.9 Evoked recorded vs simulated. 5 Hz. The dotted lines represent the time interval of stimulation artifacts. The simulated responses were built from a system model of order 5 created from the evoked potentials from 20 Hz stimulation. It is clearly seen in the recorded evoked potentials that the signals do not return to a resting state. This makes the data set unfit for this the Markov parameter realisation algorithm and this is why the error is large.

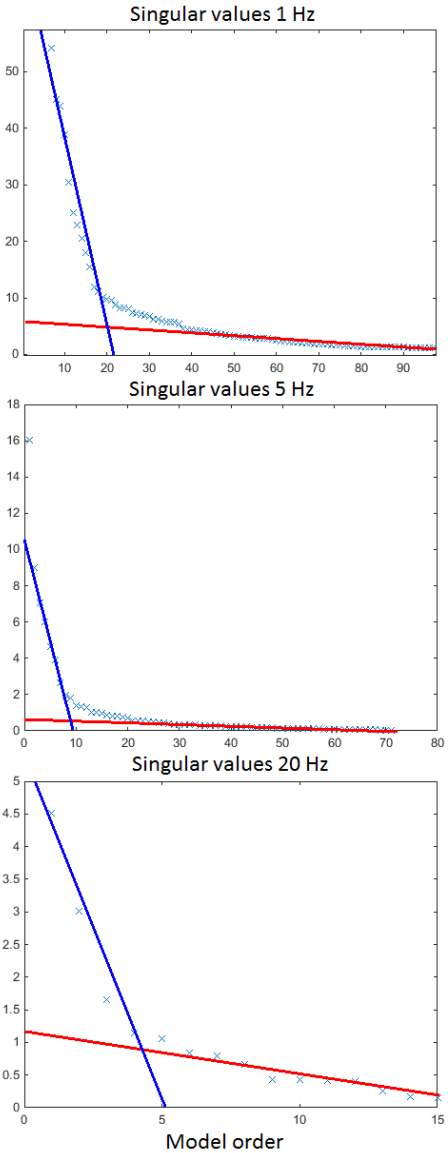

Figure 5.10 The singular values from the Σ matrix in the singular value decomposition in the three different system models. The 1 Hz singular values have been zoomed in to give a clearer view. The intersection of the lines were used to find the order of the systems, the blue can be seen as valid system variables and the red as noise or other disturbances that is undesirable and was excluded from the models.

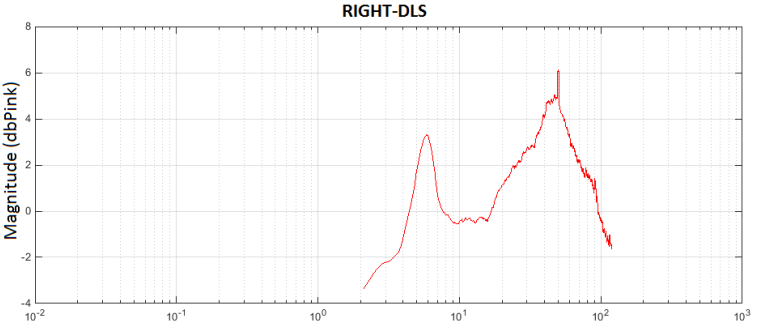

(a)

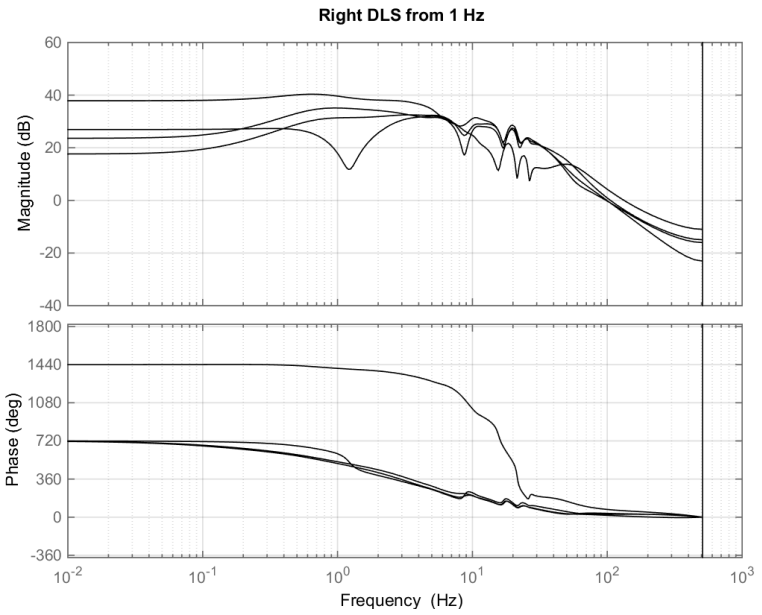

(b)

Figure 5.11 a) The PSD of the RIGHT-DLS structure. b) The magnitude Bode diagram from the channels in the 1 Hz system model that correspond to the RIGHT-DLS. Note that the magnitude on the y-axis is different in both diagrams.

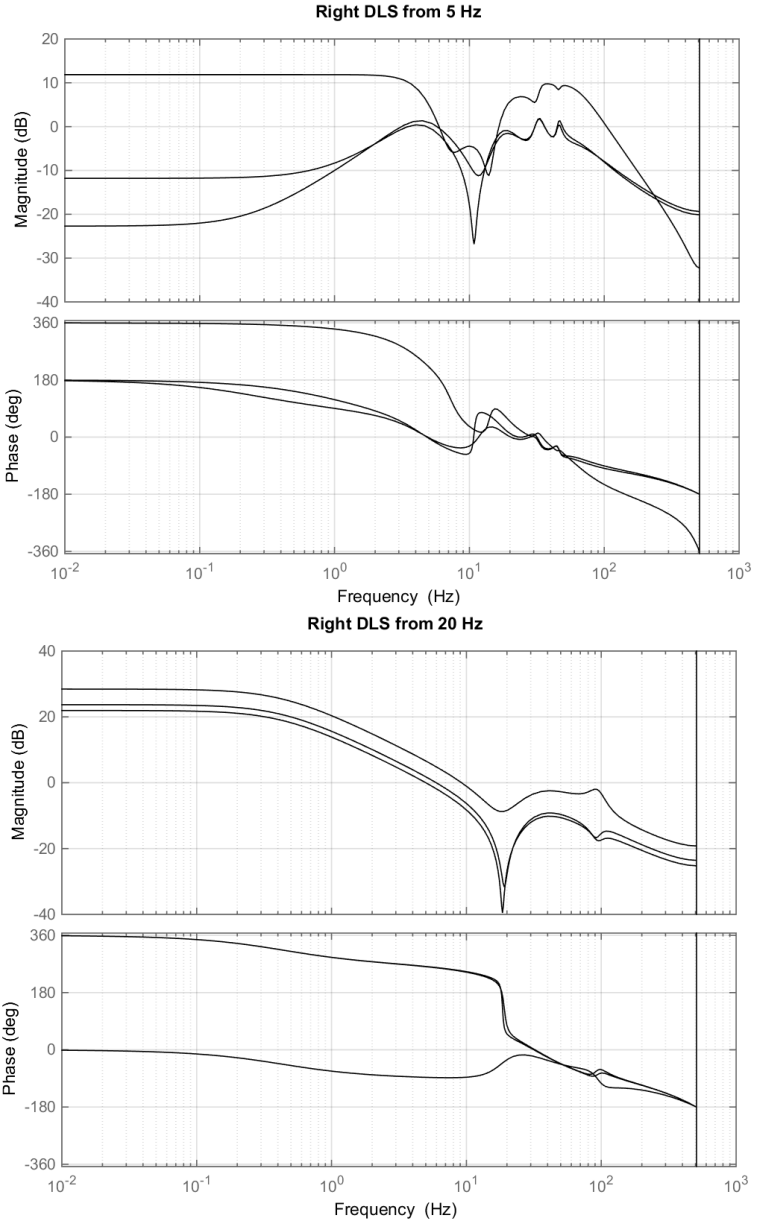

Figure 5.12 The Bode diagrams from the channels in the 5 and 20 Hz system models that correspond to the RIGHT-DLS. Note that the magnitude on the y-axis is different in both diagrams.

6

Discussion

6.1 Categorising data and power spectral densities

The animal was deemed a good example of 6-OHDA lesions and displayed parkinsonian motor symptoms, clear visual symptoms was observed while the animal was under the influence of Levodopa (L-dopa) induced dyskinesia. The local field potentials (LFPs) confirmed this. Many parkinsonian oscillations could be seen in the power spectral density diagrams, seen in Figure 5.2, where properties were seen that research papers have categorised as parkinsonian. The lesioned hemisphere which have a lack of dopamine displays a lower activity in the 35-50 Hz area than the intact hemisphere. And, when introduced to L-dopa a broad banded increase could be seen in those same frequencies, this because it caused L-dopa induced dyskinesia which adds muscle movements and with more movement, more activity. There were clear distinctions between parkinsonian, health and L-dopa induced dyskinetic data. That this could be so clearly seen feels like a step in the right direction for further research where maybe power density diagrams (PSDs) could be used for adaptive deep brain stimulation (aDBS), effects on the PSDs from the stimulation could then be further studied.

6.2 Evoked potentials

As seen in the field powers, the dyskinetic states do not produce as strong reactions to the deep brain stimulation as the parkinsonian state do. It can be speculated that this may be because the dyskinetic state interferes with the stimulus and therefore, responses are harder to produce which agrees with the observations in the threshold testing where no visual responses were seen in the dyskinetic state.

6.3 Peristimulus time histograms

The choice of having the reticular thalamus (RT) as the stimulus target proved to be an interesting one. Clear visual behavioural responses to the stimulation seemed

very promising but that no visual responses to the stimulation were seen during L-dopa induced dyskinesia could mean that there were not much to gain from those data sets. Delving through the data and the peristimulus time histograms (PSTHs) some effects could be seen. However, as a response to the stimulus pulse the basal ganglia and cortex displayed peaks and valleys in activity, the peaks reoccurring with 5-10 Hz for about half a second after the pulse in most structures. While the data in the lesioned hemisphere lacked most structures, and only finding neurons in the striatum, these still seemed to provide the same oscillations as could seen in the healthy hemisphere. It can be speculated that an explanation to these peaks of activity that occur with 5-10 Hz frequency might be that the interaction between the thalamus and RT is put into an oscillatory state. The stimulation pulse excites the RT making it send a strong inhibitory signal to the thalamus, almost silencing it. The thalamus though is usually sending excitatory signals to the RT and with them gone silent the RT gets a bit weaker and that lessens the inhibitory signals from the RT to the thalamus and so on, this also setting the whole basal ganglia in motion. The left thalamus was the only structure reacting to the stimulation by being silenced, dropping its firing rate to zero. Since the RT is inhibiting the thalamus (seen in Figure 2.2(b)) this effect can be expected since there are papers pointing towards that the RT connects to thalamus in both hemispheres [Raos and Bentivoglio, 1993] possibly explaining this valley of activity in the thalamus contralateral to the stimulus.

6.4 Markov model responses, order and Bode diagrams

The evoked potentials were accurately recreated for the models based on 1 Hz stimulation frequency. The evoked potentials from the 5 Hz stimulation frequencies were not as accurate as the 1 Hz model and the model based on the evoked potentials from the 20 Hz did not recreate them accurately. One explanation may be that for the 20 Hz evoked potentials the responses did not have time to go back to a resting state making them unsuitable for the algorithm. It is interesting that the order of the system decreased with an increase in stimulation frequency and it can be speculated that the reason behind this is because when applying a higher stimulation the inhibition from stimulus in the RT get continuously applied instead of having time to get into the oscillatory 5-10 Hz state previously discussed and thus the slower stimulation frequency would have time to be more complex. Then a follow-up question can be for which maximum frequency this can be observed? Is there an even faster frequency in which the inhibition can be so strong that the response again can have time to go back to a resting state between pulses? It would be interesting to investigate this aspect further up to frequencies usually used in open-loop DBS like 130 Hz and see if this phenomena can be seen in other frequency ranges. Since the evoked potentials from 1 Hz and 5 Hz stimulation are so different there might also be an effect called phase locking affecting the responses. In phase locking the neurons

get stuck at firing at a delay related to the stimulation frequency. This could be investigated using a pseudo random stimulation sequence, meaning that the stimulus pulses would not come with a specific frequency but be almost random with control over the closest two pulses could be and the sequence having the same properties as white noise, this would probably at least reduce the phase locking if there is one. Doing that with a closest interval over a second would probably reveal a "true" impulse response. The Bode diagrams show some trending similarities with the PSD from the parkinsonian state which may indicate that the stimulus-response model is on the right track. However, the similarities are limited to general trends of the plot and it is not clear that one can validate the other. According to [Kringelbach et al., 2010], a parkinsonian state could be indicated by having an increase in the 11-30 Hz band. This was seen in one out of three channels in the model based on 1 Hz evoked where a gain was present in that region.

6.5 Improving results

Artifacts

When the stimulation pulse is applied to the system, the added current will try to spread out as much possible and to reach an equilibrium or steady state. This effect may not be fast enough to ignore during the modelling of the system and may affect the evoked potentials. The effect observed with an oscilloscope looked like an exponential shaped equalisation back to the zero state. The way the artifact was categorised here is via the PSTH diagram in which an artifact is seen to be around 5 ms long. However, this is an uncertainty and the length, shape and form of the artifact should be investigated further, maybe looking into studying responses of a stimulation pulse in a substance similar to brain cells or even use brains extracted from previous testing animals. If the artifact could be identified that opens up a lot of different methods and techniques to remove it such as template matching.

Testing

The stimulation target should be considered. While RT was interesting and seemed to affect both hemispheres, no signs of decreased parkinsonian symptoms were observed during the threshold testing so a more tested stimulation target like the subthalamic nucleus (STN) or globus pallidus (GP) would be good choices to include in further research to be able to compare different stimulation targets. Also, the use of pseudo random stimulation paradigms instead of 1 Hz or similar would be a good way to check if phase locking occurs or not. Checking a large variety of stimulation frequencies would also be interesting to investigate.

Bootstrap and time stamps

During the process of finding the time stamps there was a manual aspect of identifying a correct one, then that one was used to create a template. The template was

used as a comparison around all the other time stamps to find out if they needed to be shifted. A good way to improve the accuracy of this identification would be to use the evoked potential calculated with these time stamps as the template in an additional run with the method to bootstrap the script (use the result of a method to calculate new improved results with the same method).

More animals

A finding in one animal is just an observation, to be able to verify whether the model is good or not the procedure could be standardised and multiple testing animals used to produce more reliable results.

Noise

In the PSDs 50 Hz power line noise is observed. In this laboratory environment the 50 Hz noise is not uncommon in the recorded data since the measured signals are weak and it takes some electronic equipment to acquire them. If needed, a way to reduce this is to set up a Faraday's cage around the animals open-field environment.

6.6 Alternative methods

The Markov realisation method focused on being able to identify the brain of the testing animal as a stimulus-response model. If this approach was successful it would be possible to manipulate the LFPs of the recorded channels. There are alternative methods of implementing aDBS. In one papers, researchers looked at the action potentials in certain structures (for example GP) and when one was observed a train of stimulation pulses (7 pulses with 130 Hz) was sent [Rosin et al., 2011]. Another paper looked at the PSD created in real time from the LFPs and enabling a stimulation protocol when peaks in the beta band in the PSD were above a set threshold [Little et al., 2013]. Since a peak in the beta band was observed in Figure 4.9 before the injection of L-dopa this method could be interesting to try together with the 6-OHDA rat model of PD.

6.7 Objectives and comments

The objectives included to categorise parkinsonian, L-dopa induced dyskinesia and health data. Differences were found in the form of power density plots where clear distinctions between the different states could be seen. A testing protocol was determined but it can be developed further by increasing the number of tested stimulation frequencies and also including a pseudo random pattern in the stimulation. Regarding the objective of investigating RT as a stimulus target, here it has been shown that stimulus in the RT affects both hemispheres and that the responses differ when comparing parkinsonian and dyskinetic states. The final objective was to determine

a system model for automatic control. While a system model was determined, its similarities with the parkinsonian rat brain remain to be fully explored. The system model performed well in producing similar evoked potentials/impulse responses for low frequencies but its Bode diagram only displayed general trends that could be compared with the power spectral diagrams from the parkinsonian rat brain.

6.8 Conclusion

The title of this thesis is impulse response analysis of neuromodulation for the treatment of motor symptoms in Parkinson's disease and the aim was to investigate a LFP-based model of the basal ganglia created from Markov parameter realisation. If a dependable model could be found, that opens up for the studying of the next step. Which, would be to put this model into a closed loop together with a controller and face the challenge of finding a suitable control parameter. Where should it be located?, how many are needed?, which format should be used? plus tackling the issue of stimulation artifacts that the control parameter might be subjected to. Because, if that model is controllable and can be used to reduce the unwanted parkinsonian features, it should be possible to reduce the same features in the basal ganglia. Here it was discovered that depending on which stimulation protocol was used, the evoked potentials produced were different. The Markov parameter realisation is based on the impulse response (here evoked potentials) and the A, B and C matrices also changed when the stimulation protocol changed. Therefore, a dependable model was not found here, but instead suggestions of what further research that would have an increased chance to find it. None of the models created from the stimulation protocols displayed a bode diagram with suppression in the 20 Hz or 80 Hz frequency range which are closely related to parkinsonian motor symptoms and L-dopa induced dyskinesia respectively which could have indicated that the stimulus protocols were well suited for reducing those symptoms. RT is a new stimulus target for treatment of parkinsonian motor symptoms and here it has been shown that as a stimulation target it shows some interesting qualities, such as affecting both hemispheres and that it can put the basal ganglia in a 5-10 Hz oscillatory activity. Also, that different responses are produced with different stimulation protocol. These changes are very interesting and here it is concluded that RT should be further researched as a stimulus target. The answers to the following questions are probably very interesting, at which stimulation frequencies do these changes of the system occur? are they really frequency bound? do they eventually stop? Further research here is encouraged.

Appendix

State space representation

In the following pages state space representation of the three calculated system models are shown. The values have been rounded to two decimals. The indexes 1, 5 and 20 indicate from which stimulus protocol the systems were created. 1 from the impulse response (evoked potentials) to the 1 Hz stimulation protocol, 5 from the 5 Hz protocol and 20 from 20 Hz protocol.

$$A_1 = 0.01 \cdot \begin{bmatrix}
100 & 2 & 0 & 0 & 0 & 1 & 0 & 0 & 0 & 1 & 0 & 0 & 0 & 0 & 0 & 0 & 0 & 0 & 0 & 0 \\
-2 & 99 & -2 & 2 & 0 & 0 & 0 & 0 & 0 & -1 & 0 & 0 & 0 & 0 & 0 & 0 & 0 & 0 & 0 & 0 \\
1 & 2 & 99 & 0 & 2 & -1 & 0 & -1 & 1 & -2 & 0 & -2 & -1 & 0 & 0 & 0 & 0 & 0 & 0 & 0 \\
-1 & -2 & 2 & 99 & -2 & 1 & 0 & 1 & -1 & 2 & 0 & 2 & 1 & 0 & 0 & 0 & 0 & 0 & 0 & 0 \\
0 & 0 & -2 & 2 & 100 & -4 & 0 & 0 & 0 & 0 & 0 & 0 & 0 & 0 & 0 & 0 & 0 & 0 & 0 & 0 \\
-1 & -1 & 3 & -4 & 5 & 97 & 0 & 0 & -3 & -1 & 0 & 3 & 1 & -1 & 1 & 2 & -1 & 1 & 0 & 2 \\
0 & 0 & 0 & 0 & 0 & 1 & 99 & -11 & 0 & 0 & 0 & 0 & 0 & 0 & 0 & 0 & 0 & 0 & 0 & 0 \\
0 & 0 & 1 & -2 & 0 & -2 & 11 & 99 & -2 & -1 & 0 & 0 & 0 & 0 & 0 & 1 & -1 & 1 & 0 & 1 \\
0 & 1 & -1 & 1 & 0 & 3 & 0 & 2 & 98 & -12 & 1 & 0 & 0 & -1 & 1 & 0 & 1 & 0 & 0 & 1 \\
-1 & -1 & 2 & -2 & 1 & -4 & 1 & -2 & 13 & 95 & -1 & 0 & -1 & -1 & 0 & 4 & -4 & 2 & -1 & 3 \\
0 & 0 & -1 & 1 & 0 & 1 & 0 & 1 & -1 & 4 & 99 & -5 & -1 & -1 & 1 & -2 & 2 & -1 & 0 & 0 \\
-1 & -1 & 2 & -2 & 1 & -5 & 1 & -2 & 3 & -9 & 8 & 91 & -1 & 5 & -6 & 2 & -7 & 2 & -2 & 0 \\
0 & 0 & 1 & -1 & 0 & -2 & 0 & -1 & 1 & -3 & 2 & -7 & 98 & 3 & -3 & 2 & -3 & 1 & -1 & 1 \\
0 & 0 & 1 & -1 & 0 & -1 & 0 & -1 & 1 & -3 & 2 & -9 & -6 & 98 & -8 & 6 & -1 & 1 & -1 & 4 \\
0 & 0 & 0 & 0 & 0 & 1 & 0 & 1 & -1 & 2 & -1 & 8 & 4 & 11 & 98 & -6 & 1 & -1 & 0 & -3 \\
0 & -1 & 1 & -1 & 0 & -2 & 0 & -1 & 1 & -6 & 2 & -9 & -5 & -8 & 9 & 93 & -2 & -3 & 0 & -4 \\
0 & 1 & -1 & 1 & 0 & 2 & 0 & 1 & -1 & 5 & -2 & 10 & 5 & 5 & -4 & 13 & 92 & 3 & 2 & -7 \\
0 & 0 & 1 & -1 & 0 & -1 & 0 & -1 & 1 & -3 & 1 & -6 & -3 & -3 & 3 & -6 & 8 & 96 & -7 & 2 \\
0 & 0 & 0 & 0 & 0 & 1 & 0 & 1 & 0 & 2 & 0 & 4 & 2 & 2 & -2 & 5 & -9 & 12 & 97 & -7 \\
0 & -1 & 1 & -1 & 0 & -2 & 0 & -1 & 1 & -4 & 2 & -6 & -4 & -4 & 5 & -8 & 17 & -12 & 16 & 88
\end{bmatrix}$$

$$B_1 = 0.01 \cdot \begin{bmatrix} 116 & 127 & -100 & 105 & -37 & 145 & -16 & 54 & -52 & 107 & -34 & 111 & 45 & 33 & -26 & 53 & -48 & 35 & -22 & 46 \end{bmatrix}^T$$

$$C_1 = 0.01 \cdot \begin{bmatrix}
12 & 4 & 47 & -36 & -9 & -49 & -2 & 1 & -24 & 13 & -10 & 55 & 15 & -11 & 8 & 15 & 14 & -2 & 2 & 24 \\
18 & -4 & 24 & -31 & -3 & -54 & 6 & -5 & -3 & 2 & 11 & 49 & 12 & 2 & -3 & 25 & -3 & 2 & 6 & 0 \\
39 & -52 & -33 & 10 & 17 & -27 & 4 & -15 & -7 & -31 & 7 & -11 & -5 & -14 & 8 & 19 & -7 & 8 & -8 & 17 \\
39 & -52 & -33 & 10 & 17 & -27 & 4 & -15 & -7 & -31 & 7 & -11 & -4 & -14 & 8 & 19 & -7 & 8 & -8 & 17 \\
4 & 21 & 45 & -54 & -4 & -47 & -1 & 2 & -29 & 14 & -9 & 53 & 15 & -14 & 15 & 11 & 27 & -6 & -8 & 23 \\
45 & -44 & -13 & 19 & 5 & -40 & 2 & -21 & -10 & -40 & 5 & -19 & -14 & -15 & 14 & 8 & -5 & 5 & -1 & 14 \\
4 & 6 & 21 & -25 & -8 & -41 & 6 & -5 & 8 & 0 & 12 & 25 & 25 & 9 & -5 & 24 & -15 & 14 & -2 & 3 \\
10 & 16 & 40 & -49 & -12 & -53 & -2 & 0 & -10 & 22 & 7 & 49 & 11 & 3 & 10 & 1 & 10 & -5 & 13 & 6 \\
48 & -45 & -21 & 31 & 4 & -34 & -1 & -25 & -14 & -44 & 7 & -26 & -16 & -12 & 14 & 12 & -10 & 7 & -4 & 12 \\
37 & -39 & -8 & 7 & 5 & -43 & 5 & -22 & -2 & -37 & 5 & -4 & -6 & 3 & -2 & 26 & -20 & 15 & -3 & 8 \\
47 & -46 & -14 & 25 & 0 & -43 & -2 & -26 & -13 & -47 & 7 & -27 & -17 & -13 & 11 & 12 & -16 & 10 & -3 & 15 \\
44 & -46 & -7 & 18 & -1 & -45 & -2 & -23 & -14 & -41 & 4 & -17 & -11 & -8 & 7 & 18 & -23 & 15 & -5 & 18
\end{bmatrix}$$

$$A_5 = 0.01 \cdot \begin{bmatrix} 89 & -19 & -4 & 5 & 19 & -4 & 1 & -1 & 1 & -1 \\ 18 & 98 & -1 & 1 & 3 & -1 & 0 & 0 & 0 & 0 \\ 6 & 0 & 100 & -2 & 0 & 1 & -1 & 1 & 0 & 0 \\ -7 & 0 & 4 & 98 & -3 & 3 & 1 & -1 & 2 & -1 \\ -20 & 2 & 3 & -16 & 66 & -4 & -3 & -1 & 5 & -6 \\ 3 & 0 & -2 & 0 & 23 & 96 & -4 & -1 & -3 & 2 \\ -2 & 0 & 0 & -5 & -10 & 10 & 97 & -13 & -5 & -10 \\ 1 & 0 & -1 & 1 & 9 & -2 & 16 & 97 & -18 & 2 \\ -1 & 0 & -1 & -3 & -8 & 7 & 2 & 20 & 96 & -18 \\ 1 & 0 & -2 & 1 & 14 & -3 & 16 & -2 & 23 & 92 \end{bmatrix}$$

$$B_5 = 0.01 \cdot \begin{bmatrix} -143 & -10 & 15 & -48 & -131 & 29 & -21 & 11 & -10 & 19 \end{bmatrix}^T$$

$$C_5 = 0.01 \cdot \begin{bmatrix} -61 & -4 & 0 & 17 & 58 & -7 & 1 & 4 & -3 & -5 \\ -16 & -2 & 0 & 0 & 7 & -4 & 0 & -2 & 2 & 3 \\ -24 & -3 & 8 & -1 & 14 & -10 & 10 & -9 & 8 & -2 \\ -9 & -1 & 1 & -2 & -4 & 1 & -1 & 1 & 0 & 3 \\ -9 & -2 & 0 & -3 & -3 & -1 & -1 & -1 & 1 & 3 \\ -57 & -1 & 5 & 12 & 53 & -15 & 7 & -2 & 1 & 3 \\ -11 & -3 & 1 & -3 & -2 & -1 & -2 & 0 & 1 & 2 \\ -31 & -2 & 8 & 3 & 34 & -10 & 6 & -1 & -1 & -9 \\ -68 & 2 & -2 & 15 & 54 & -14 & 5 & -1 & 0 & 5 \\ -7 & -1 & 0 & -3 & -4 & 1 & -2 & 1 & 0 & 2 \\ -48 & 1 & -3 & 10 & 48 & -12 & 6 & -5 & -1 & 3 \\ -11 & -3 & 1 & -3 & -3 & -1 & -1 & -1 & 2 & 3 \\ -58 & 7 & -2 & 16 & 57 & -11 & 5 & -2 & -2 & -1 \\ 18 & -6 & 8 & 11 & 19 & -15 & 10 & -6 & 0 & 5 \\ 11 & 0 & 8 & 19 & -2 & -15 & 6 & 2 & -9 & 5 \\ 18 & -6 & 8 & 11 & 19 & -15 & 10 & -6 & 0 & 5 \\ -1 & -3 & 0 & -15 & 1 & 4 & 20 & -5 & 4 & 1 \end{bmatrix}$$

$$A_{20} = 0.01 \cdot \begin{bmatrix} 102 & 6 & -1 & 5 & -1 \\ 10 & 82 & -15 & -7 & 0 \\ 1 & 28 & 92 & 21 & 5 \\ -8 & 12 & -37 & 80 & 26 \\ 3 & 18 & 4 & -61 & 71 \end{bmatrix} \quad B_{20} = 0.01 \cdot \begin{bmatrix} -85 \\ 113 \\ -39 \\ -44 \\ -36 \end{bmatrix}$$

$$C_{20} = 0.01 \cdot \begin{bmatrix} -49 & 52 & -23 & 20 & -4 \\ -5 & 9 & 0 & 0 & -1 \\ -8 & 14 & -3 & 4 & 3 \\ -3 & 6 & -1 & -3 & -3 \\ -2 & 5 & 0 & -1 & -2 \\ -32 & 38 & 13 & 4 & -1 \\ -3 & 7 & 0 & -2 & -2 \\ 12 & 11 & -10 & 10 & 0 \\ -43 & 64 & 10 & 6 & -3 \\ -2 & 4 & 0 & -2 & -2 \\ -21 & 28 & 11 & 2 & -6 \\ -4 & 7 & 0 & -2 & -3 \\ -17 & 25 & 2 & 3 & 0 \\ 4 & -27 & -4 & 15 & 15 \\ 6 & -16 & -23 & 8 & 13 \\ 4 & -26 & -4 & 15 & 14 \\ -35 & -6 & -5 & -4 & 6 \end{bmatrix}$$

Bibliography

Ballabh, P., A. Braun, and M. Nedergaard (2004). "The blood-brain barrier: an overview: structure, regulation, and clinical implications." *Neurobiology of disease* **16**:1, pp. 1–13.

Cenci, M. A. and M. Lundblad (2007). "Ratings of L-DOPA-induced dyskinesia in the unilateral 6-OHDA lesion model of Parkinson's disease in rats and mice." *Current protocols in neuroscience* October, Unit 9.25.

Dash, P. (1997). *"Neuroscience Online: An Electronic Textbook for the Neurosciences | Department of Neurobiology and Anatomy"*. [Online Book]. Chap. 11. URL: `http://neuroscience.uth.tmc.edu/s4/chapter11.html` (visited on 08/18/2015).

Fee, M. S., P. P. Mitra, and D Kleinfeld (1996). "Automatic sorting of multiple unit neuronal signals in the presence of anisotropic and non-Gaussian variability." *Journal of neuroscience methods* **69**:2, pp. 175–188.

Halje, P., M. Tamtè, U. Richter, M. Mohammed, M. A. Cenci, and P. Petersson (2012). "Levodopa-induced dyskinesia is strongly associated with resonant cortical oscillations." *The Journal of neuroscience : the official journal of the Society for Neuroscience* **32**:47, pp. 16541–51. URL: `http://www.jneurosci.org/content/32/47/16541`.

Ho, B. L. and R. E. Kalman (1966). "Effective construction of linear state-variable models from input/output functions". *Regelungstechnik* 14, pp. 545–548.

Johansson, R. (2012). *"System Modeling and Identification"*.

Kim, S. J., J. Y. Sung, J. W. Um, N. Hattori, Y. Mizuno, K. Tanaka, S. R. Paik, J. Kim, and K. C. Chung (2003). "Parkin Cleaves Intracellular α-Synuclein Inclusions via the Activation of Calpain". *Journal of Biological Chemistry* **278**:43, pp. 41890–41899.

Kringelbach, M. L., A. L. Green, S. L. F. Owen, P. M. Schweder, and T. Z. Aziz (2010). "Sing the mind electric - principles of deep brain stimulation." *The European journal of neuroscience* **32**:7, pp. 1070–9.

Leevanjackson (2009). *File:Basal Ganglia and Related Structures.svg - Wikimedia Commons*. (Visited on 06/25/2015).

Little, S., A. Pogosyan, S. Neal, B. Zavala, L. Zrinzo, M. Hariz, T. Foltynie, P. Limousin, K. Ashkan, J. FitzGerald, A. L. Green, T. Z. Aziz, and P. Brown (2013). "Adaptive deep brain stimulation in advanced Parkinson disease." *Annals of neurology* **74**:3, pp. 449–57.

Merrill, D. R., M. Bikson, and J. G. R. Jefferys (2005). "Electrical stimulation of excitable tissue: Design of efficacious and safe protocols". *Journal of Neuroscience Methods* **141**:2, pp. 171–198.

Multi Channel Systems (MCS) (2012). *MC_Stimulus II Multichannel Systems Software*. URL: `http://www.multichannelsystems.com/software/mc-stimulus-ii`.

Olanow, C. W., J. A. Obeso, and F. Stocchi (2006). "Drug insight: Continuous dopaminergic stimulation in the treatment of Parkinson's disease." *Nature clinical practice. Neurology* **2**:7, pp. 382–92.

Parkinson's Disease Foundation (PDF) (2015a). *"Surgical Treatments"*. URL: `http://www.pdf.org/en/surgical_treatments` (visited on 11/02/2015).

Parkinson's Disease Foundation (PDF) (2015b). *"What is Parkinson's Disease?"*. URL: `http://www.pdf.org/about_pd` (visited on 02/26/2015).

Priori, A., G. Foffani, L. Rossi, and S. Marceglia (2013). "Adaptive deep brain stimulation (aDBS) controlled by local field potential oscillations". *Experimental Neurology* **245**, pp. 77–86.

Purves, D. (2004). *"Neuroscience Third Edition"*. Chap. 17: Modulation of Movement by the Basal Ganglia, p. 773.

Raos, V and M Bentivoglio (1993). "Crosstalk between the two sides of the thalamus through the reticular nucleus: a retrograde and anterograde tracing study in the rat." *The Journal of comparative neurology* **332**:2, pp. 145–54.

Redgrave, P., M. Rodriguez, Y. Smith, and M. C. Rodriguez-oroz (2010). "UKPMC Funders Group Goal-directed and habitual control in the basal ganglia : implications for Parkinson ' s disease". *Nature Publishing Group* **11**:11, pp. 760–772.

Rosin, B., M. Slovik, R. Mitelman, M. Rivlin-Etzion, S. N. Haber, Z. Israel, E. Vaadia, and H. Bergman (2011). "Closed-loop deep brain stimulation is superior in ameliorating parkinsonism". *Neuron* **72**:2, pp. 370–384.

Lund University
Department of Automatic Control
Box 118
SE-221 00 Lund Sweden

Document name
MASTER´S THESIS

Date of issue
June 2016

Document Number
ISRN LUTFD2/TFRT--5993--SE

Author(s)
Staffan Hedström

Supervisor
Per Petersson, Biomedical Centre, Lund University, Sweden
Bo Bernhardsson, Dept. of Automatic Control, Lund University, Sweden
Rolf Johansson, Dept. of Automatic Control, Lund University, Sweden (examiner)

Sponsoring organization

Title and subtitle

Impulse response analysis of neuromodulation for the treatment of motor symptoms in Parkinson's disease

Abstract

In adaptive deep brain stimulation, a treatment for motor symptoms in Parkinson's disease, the target of the stimulus is usually in the sub-thalamic nucleus or the globus pallidus. In this thesis, a new stimulus target called reticular thalamus is investigated in a rat model of Parkinson's disease. The responses to the stimulus were recorded from both local field potentials and action potentials from neurons in a live animal implanted with an electrode array and stimulus electrode. The local field potentials were used to investigate the state of a rat, to categorise healthy, parkinsonian and dyskinetic states, to create a response to the stimulus used for investigating the effects of the new stimulus target and to try find the transfer function (turns input into output) to the brain of a rat model of Parkinson's disease with the Markov parameter realisation algorithm. The new stimulus target showed interesting and clear visual responses from the rat and set the structures in the basal ganglia in a 5-10 Hz ringing for half a second as revealed by a peristimulus time histogram. A power spectral density diagram revealed characteristics previously shown to be correlated with Parkinson's disease. The transfer function created from the responses was not able to predict the responses to other stimulation protocols other than the one used to build the transfer function, possibly due to the fact that the stimulus target was more effectively inhibited by the higher frequency stimulus protocols, so that the biological properties changed the system.

Keywords

Classification system and/or index terms (if any)

Supplementary bibliographical information

ISSN and key title
0280-5316

ISBN

Language
English

Number of pages
1-54

Recipient's notes

Security classification